AEDC-TR-71-181

cy 2

TWO-DIMENSIONAL FLOW CALCULATIONS IN THE ELECTRIC FIELD PLANE FOR LINEAR MHD CHANNELS

Paul W. Johnson
ARO, Inc.

September 1971

PROPULSION WIND TUNNEL FACILITY
ARNOLD ENGINEERING DEVELOPMENT CENTER
AIR FORCE SYSTEMS COMMAND
ARNOLD AIR FORCE STATION, TENNESSEE

NOTICES

When U. S. Government drawings specifications, or other data are used for any purpose other than a definitely related Government procurement operation, the Government thereby incurs no responsibility nor any obligation whatsoever, and the fact that the Government may have formulated, furnished, or in any way supplied the said drawings, specifications, or other data, is not to be regarded by implication or otherwise, or in any manner licensing the holder or any other person or corporation, or conveying any rights or permission to manufacture, use, or sell any patented invention that may in any way be related thereto.

Qualified users may obtain copies of this report from the Defense Documentation Center.

References to named commercial products in this report are not to be considered in any sense as an endorsement of the product by the United States Air Force or the Government.

TWO-DIMENSIONAL FLOW CALCULATIONS IN THE ELECTRIC FIELD PLANE FOR LINEAR MHD CHANNELS

Paul W. Johnson
ARO, Inc.

FOREWORD

The work reported herein was sponsored by Headquarters, Arnold Engineering Development Center (AEDC), Air Force Systems Command (AFSC), under Program Element 62405334, Project 8950.

The results of this research were obtained by ARO, Inc. (a subsidiary of Sverdrup & Parcel and Associates, Inc.), contract operator of AEDC, AFSC, Arnold Air Force Station, Tennessee, under Contract F40600-72-C-0003 from July 5, 1966, to June 30, 1970, under ARO Projects PW5704, PW3804, and PW3004. The manuscript was submitted for publication on June 14, 1971.

A special acknowledgement is accorded to Leon E. Ring whose contributions included the derivation of the formulas for the conservation of mass, conservation of current, the thermodynamic functions, and the suggestion of the streamtube method of analysis. Recognition is also accorded to Joyce Iannuzzi for having assisted in the derivation of the thermodynamic functions of nitrogen.

This technical report has been reviewed and is approved.

Ules L. Barnwell
Major, USAF
Research and Development Division
Directorate of Technology

Robert O. Dietz
Acting Director
Directorate of Technology

ABSTRACT

The two-dimensional, steady, compressible, inviscid flow of ionized gas through linear, segmented electrode, magnetohydrodynamic (MHD) channels is computed in the plane of the applied electric field. The solutions obtained for the gas dynamic and electrical quantities satisfy the coupled fluid mechanical conservation laws and Maxwell's equations at all points of the flow field simultaneously. The nonuniform profiles which are obtained include the effects of transverse variations in incoming gas dynamic profiles, local Hall currents in Faraday channels, transverse currents in Hall devices, and axial magnetic field gradients.

CONTENTS

APPENDIXES

Page

VIII. TABLES

NOMENCLATURE

A	Channel cross-sectional area, m^2
a	Speed of sound, m/sec
$\vec{B}$	Magnetic induction, tesla
C_p	Coefficient of specific heat at constant pressure, $m^2/(sec^2\text{-}°K)$
d	Channel width between conducting walls, m
$\vec{E}$	Electric field measured in laboratory coordinate frame of reference, v/m
$\vec{E}^*$	Electric field measured in moving fluid frame of reference, v/m
H	Total enthalpy, m^2/sec^2
h	Static enthalpy, m^2/sec^2
$\vec{j}$	Current density, amp/m^2
M	Mach number
$\dot{m}$	Mass flow rate, kg/sec
p	Static pressure, $Newton/m^2$
p_o	Stagnation pressure, $Newton/m^2$
p_o'	Total pressure behind normal shock, atm
q	Magnitude of velocity vector, m/sec
R	Gas constant, $m^2/(sec^2\text{-}°K)$
S	Entropy, $m^2/(sec^2\text{-}°K)$

S_w	Seed rate by weight
s, n	Natural coordinates measured tangential and normal to particle paths
T	Temperature, °K
t	Time, sec
u, v, w	Velocity components, m/sec
$\vec{V}$	Velocity, m/sec
V_y	Voltage difference between conductor walls, v
W	Channel height between insulating walls, m
x	Axial coordinate, m
y	Transverse coordinate in plane of applied electric field, m
Z	Compressibility of gas
z	Transverse coordinate in plane of applied magnetic field, m
ρ	Density of gas, kg/m^3
σ	Electrical conductivity of gas, mho/m
ϕ	Electric potential defined by Eq. (VI-1), v
Ψ	Electric current stream function, defined by Eq. (II-4)
ψ	Mass stream function, defined by Eq. (5)
$\omega\tau$	Hall parameter

SUBSCRIPTS

avg	Average value. Total enthalpy is mass averaged; all other variables are spatially averaged in the y direction
i, j	Values of variables on ith and jth streamlines
s, n	Vector components tangential and normal to streamlines
x, y, z	Vector components in the directions of the cartesian coordinates
∞	Standard atmospheric value

OTHER

[ ]	Vector box product

SECTION I
INTRODUCTION

The channel flow of an electrically conducting gas has been of engineering interest in recent years because of the capability of producing an electromagnetic interaction with the fluid which results in either energy addition to or extraction from the flow, thus causing an acceleration of the fluid or a generation of electrical power. In order to make theoretical predictions of the performance of these devices, previous investigators introduced assumptions to obtain tractable formulations which led to analytical models at some variance to their physical counterparts. Representative of these approaches are the solutions discussed in Ref. 1. These include exact solutions to certain simplified, linearized versions of the magnetohydrodynamic (MHD) equations (Chapter 10 of Ref. 1), and a discussion of numerical solutions to approximations of the describing equations (Chapter 11 of Ref. 1). The numerical cases considered there utilize the quasi-one-dimensional approximation to MHD channel flow. Another type of analytical model which has been studied is exemplified by Ref. 2 in which the two-dimensional, compressible, laminar boundary layer form of the equations of motion are solved across the entire channel in the E-plane. There the assumptions are made that the gas obeys an ideal equation of state, the insulator walls are parallel, the ratio of the electric field components E_y/E_x is constant, and E_x is a function only of the x coordinate. These latter two assumptions remove the requirement for solving an elliptic equation for the electrical properties. The analysis has been formulated in a very general manner in Ref. 3 where solutions have been obtained that include finite chemical reaction rates, electrical thermal nonequilibrium, thermal and concentration diffusion, electron energy relaxation, turbulent boundary layers, and a one-dimensional inviscid core. The electrical portion of the problem is solved by combining separate solutions for an electric current stream function in the inlet region, exit region, and periodic main part of Faraday accelerator channels. The geometry considered permits diverged electrode walls, and assumes parallel insulator walls.

The analysis performed in this investigation considers compressible, inviscid, two-dimensional flow between the electrode walls. The distinguishing feature of this study is that the calculation of the coupled gasdynamic and electrical variables is performed in a manner such that the fluid mechanical conservation laws and Maxwell's electrical differential equations are satisfied simultaneously throughout the entire field. In particular, this means that the solenoidal property of current density and the irrotational property of the electric field are satisfied

at all points of the flow field where electric current is flowing. The significance of this is that it is possible to observe the changing character of the current paths down the channel, which would not be possible if separate solutions to the electrical portion of the problem were obtained over portions of the flow field and then joined together. The results of this study show that there exists a nonnegligible coupling in the currents paths along the channel. The mass and current continuity equations are formulated in a manner which permits the B-walls, as well as the E-walls, to be nonparallel.

In order to demonstrate the physically realistic effects of the MHD variables being coupled together at all points of the flow field, the elliptic differential equations for electrical variables are solved throughout the portions of the channels where the magnetic field is nonzero (the B-field is assumed to extend beyond the electrically powered portions of the channels). Attempts to achieve the numerical solutions of these elliptic equations by iterative methods were unsuccessful. This was primarily a consequence of the large gradients in the unknown variables and, secondarily, a result of mixed boundary conditions in the Hall channel analysis. It was only when a direct noniterative method given in Ref. 4 was used that the solutions were effected. The results of the numerical experiments performed in the course of this study indicate that this method can be rendered stable on a gridwork limited in size only by available computer memory, in contrast to other direct methods which are subject to truncation error instabilities when the system is sufficiently large. This particular method seems to provide not only a sine qua non for problems with numerical complexities as severe as those of this study, but a more efficient technique for simpler problems than iterative methods provide.

The work described in this report was carried out with the following objectives: (1) to develop computation techniques for two-dimensional MHD channel flow, (2) to assess the utility of using quasi-one-dimensional calculations for design purposes, and (3) to test the capability of the theory to predict results which will compare favorably with available experimental data. The second objective is tested by averaging the two-dimensional results in a direction transverse to the channel centerline, and then comparing these values with those obtained from corresponding uniform profile solutions. The correspondence of the two methods of solution is established by matching the average values of the assumed two-dimensional profiles at the channel entrance to the specified one-dimensional variables characterizing the flow.

The third objective is tested by comparing theoretical predictions with available impact pressure measurements made at the exit of an

accelerator channel. Since the initial profiles entering the channel were not measured, an empirical method is employed in choosing the profiles that gives agreement with the experimental impact pressure measured in the B-field plane for a given accelerator run. The details of the method are described in Ref. 5.

SECTION II
DESCRIBING EQUATIONS AND ASSUMPTIONS

The analytical model of the MHD flow field considered is obtained by introducing simplifying assumptions into the equations that express the conservation of mass, momentum, and energy of an ionized gas flowing through crossed electric and magnetic fields. The solutions to these equations describe the flow in the plane of the applied electric field (the x-y plane), while at the same time they include the effect of diverging conductor walls since, in general, the channel dimension W in the z direction is both finite and a function of x. Thus, both dimensions, height and width, are permitted to vary with x. In order to analyze such a three-dimensional physical model with two-dimensional equations, the assumption of source flow is made (this is described in detail in Appendix II). This is supplemented with the additional gas dynamic assumptions that the flow is steady, inviscid, and nonheat-conducting. It is further postulated that the magnetic field is applied in the z direction and that the induced magnetic field is negligible; the electric field and current density vectors have components only in the x and y directions. The formulas for the variables which enter into the describing equations are discussed in the following sections.

2.1 GAS DYNAMIC FORMULAS

The fluid mechanical relationships are derived from the conservation of:

Mass (Source Flow)

$$\nabla \cdot W\rho\vec{V} = 0 \tag{1}$$

Momentum

$$\rho \frac{D\vec{V}}{Dt} + \nabla p = \vec{j}\times\vec{B} \tag{2}$$

Energy

$$\rho \frac{DH}{Dt} = \vec{E}\cdot\vec{j} \tag{3}$$

The analysis is performed using a streamtube method. For this purpose a transformation of coordinates is introduced which uses the von Mises variables (x, ψ) where ψ is a normalized stream function defined to satisfy continuity of mass and possessing the properties that ψ is constant along streamlines, and the increment in ψ between streamlines is directly proportional to the mass flow in the streamtubes they bound. The system of gas dynamic equations is closed by postulating that the streamtube slopes in the x-y plane vary linearly in the transverse direction from the centerline to the walls

$$\frac{\partial y}{\partial x}(x,\psi) = \frac{y}{\frac{d}{2}} \frac{d}{dx} \frac{d}{2} \tag{4}$$

Although the problem is solved using von Mises coordinates, several of the describing equations can be written in a more compact form by using natural coordinates in the notation. Thus, the use of s and n as subscripts indicates vector components in these directions, and gradients in these directions can be related to gradients in the von Mises coordinates from geometrical considerations.

When the assumption of steady flow is incorporated into Eqs. (1) to (3) the conservation relations are

Mass (Source Flow)

$$\frac{d\psi}{dn} = \frac{2W}{\dot{m}} \rho q \tag{5}$$

Momentum

$$\rho \frac{\partial}{\partial x} \frac{q^2}{2} + \frac{\partial p}{\partial x} = \left(\frac{\partial x}{\partial s}\right)^{-1} j_n B \tag{6}$$

$$\rho u \frac{\partial v}{\partial x} + \frac{\partial \psi}{\partial y} \frac{\partial p}{\partial \psi} = - j_x B \tag{7}$$

Energy

$$\rho u \frac{\partial}{\partial x} \left(h + \frac{q^2}{2}\right) = \vec{E} \cdot \vec{j} \tag{8}$$

Subsequent to the solution of these equations the streamline locations are determined from the integrated form of the definition of the mass stream function

$$y = \frac{\dot{m}}{2W} \int_{-1}^{\psi} \frac{d\psi}{\rho u} - \frac{d}{2} \tag{9}$$

In order to facilitate the numerical integration of the equations of motion, they are transformed into an equivalent system of equations as explained in Appendix III.

Separate calculations were performed where the inertial term $\rho u \frac{\partial v}{\partial x}$ in the transverse momentum relationship, Eq. (7), initially was included in the pressure prediction scheme and subsequently was not included. The results of the calculations were virtually insensitive to the choice of these two different assumptions, and hence all the results of this report were produced neglecting this term since it simplifies the numerical analysis.

To complete the formulation of the gas dynamic flow, relations are needed to compute the thermodynamic and the electrical transport properties of the working fluid. The accelerators considered in this report use either air or nitrogen. The generator is supplied with the products of combustion gases (toluene plus methanol; $7C_7H_8 + 2\ CH_3\ OH + 66\ O_2 + 67\ N_2$).

The thermodynamic functions derived for air and nitrogen (N_2) assume these gases to be in chemical equilibrium and include real-gas effects. They have been derived by postulating functional relationships which simultaneously satisfy a thermal equation of state and the second law of thermodynamics. Additional considerations involved in the selection of these relationships are that they should provide accurate curve fits to the exact values given in Refs. 6 and 7. The detailed results are presented in Appendix IV.

The thermodynamic functions of combustion gas products are obtained from curve fits to unpublished data computed at AEDC.

The electrical conductivity of seeded air and nitrogen is computed from the method described in Ref. 8. The method incorporates the known theoretical expressions for electrical conductivity of a singly ionized plasma in the two limiting cases of fully ionized and slightly ionized plasma into a form proposed by Lin, Resler, and Kantrowitz (Ref. 9) to approximate the conductivity (denoted by σ_o in this approximation) between these two limiting cases

$$\sigma_o^{-1} = \sigma_{en}^{-1} + \sigma_{ei}^{-1} \tag{10}$$

where σ_{en} is determined by electron-neutral collisions and σ_{ei} by electron-ion collisions. Subsequently, Demetriades and Argyropolous (Ref. 10) have developed a higher order approximation, written as

$$\sigma = \frac{\sigma_o}{1 - \Delta'} \tag{11}$$

in the notation of Ref. 8. Equation (11) is found by using Grad's 13-moment approximation to derive a generalized Ohm's law for a multicomponent, nonisothermal plasma, including temperature and pressure gradients, as a function of the electric and magnetic fields. The electrical conductivity is obtained in two successive approximations which are equivalent to the first and second approximations in the expansion of Sonine polynomials in the Chapman-Enskog approach.

The Hall parameter is computed from

$$\omega\tau = \frac{\sigma |\vec{B}|}{en_e} \tag{12}$$

where en_e is the product of electronic charge times electron number density.

The electrical conductivity and Hall parameter of a seeded combustion gas product are obtained from curve fits to unpublished data computed at AEDC.

2.2 MAGNETIC FIELD

It is assumed that the magnetic Reynolds number is sufficiently low so that no magnetic field is induced by the flow of electrical current. It is further assumed that the only nonvanishing component of the applied magnetic field vector is in the z direction, and that this component is a function of the x coordinate only. A functional relationship $\vec{B}(x)$ is determined for each channel by approximating the measured distribution with an analytical expression.

2.3 ELECTRIC FIELD AND ELECTRIC CURRENT DENSITY

The method for posing the analytical model describing the electrical variables in a given channel is determined by the manner in which the boundary conditions are prescribed. In the case of the Faraday channels the normal component of current density is specified on all the boundaries; hence, it is natural to solve a partial differential equation for a current stream function since in this formulation the boundary conditions possess the desideratum of being of the Dirichlet

type. The formulation of the current stream function equation is performed in Appendix V and the method of solution is described in Appendix VII. In the case of the Hall channel, the terminals are equipotential surfaces; it is natural to solve a differential equation for an electric potential in this application. The formulation of such an equation is performed in Appendix VI, and the method of solution is described in Appendix VII.

Subsequent to the solution of the appropriate elliptic equation for Ψ or ϕ, the electric field and current density are related through an Ohm's law. The formulas which are combined to describe the electrical portion of the problem are Faraday's law

$$\nabla \times \vec{E} = 0 \tag{13}$$

continuity of current in two-dimensional source flow (this is derived in Appendix II)

$$\nabla \cdot W\vec{j} = 0 \tag{14}$$

and an Ohm's law

$$j_s = \frac{\sigma}{1 + (\omega\tau)^2} [E_s - \omega\tau(E_n - qB)]$$

$$j_n = \frac{\sigma}{1 + (\omega\tau)^2} [E_n - qB + \omega\tau E_s] \tag{15}$$

Equation (15) implies that the total energy addition occurring in the energy Eq. (8) can be written as

$$\vec{E} \cdot \vec{j} = \frac{j_s^2 + j_n^2}{\sigma} + q\, j_n\, B \tag{16}$$

In all cases, the accelerator cathodes are assumed to be contained in the upper walls.

SECTION III
RESULTS

A series of flow-field profiles has been computed in order to demonstrate quantitatively the two-dimensional characteristics of the variables describing MHD channel flow, as well as to show the differences between two-dimensional and quasi-one-dimensional assumptions.

The two-dimensional characteristics are displayed by assuming shapes for the initial profiles of temperature and velocity, and then following the development of these profiles through the length of the channel. In addition, the integration of the equations of motion concurrently with Maxwell's equations gives the current components in the x-y plane that are induced by the interaction of the gas dynamic and electromagnetic fields.

The theoretical calculations have been carried out for flows through three accelerators and one Hall generator that are analytical models simulating channels constructed at AEDC. These will be referred to as Accelerator A, Accelerator B (a 20-MW accelerator designed for operation in the AEDC LORHO Pilot Complex; the actual slant-wall boundary conditions were approximated by those appropriate to a Faraday accelerator), and Accelerator C (described in Ref. 11). The generator calculations were performed for a linear (square cross section) device, as an approximate model of the circular cross section channel described in Ref. 12. The assumption of linearity was made because the interaction of the applied magnetic field with the flow in the circular channel produces three-dimensional effects.

3.1 FARADAY ACCELERATORS

In order to show the differences in accelerator results obtained by solving the equations of motion in one and two dimensions, the two-dimensional profiles are averaged in the transverse direction and then one-dimensional solutions are computed, using in both instances the same channel entrance values of appropriately selected variables which characterize the flow. In particular, the following initial values were matched:

Accelerator A

- Static pressure
- Mass averaged total enthalpy
- Mach number

Accelerator B

- Static pressure
- Mass averaged total enthalpy
- Mass flow

The two-dimensional computations incorporate the above matching conditions in conjunction with additional assumed conditions at the channel entrance as given in Tables I and II (Appendix VIII). For each Accelerator A and B, two cases of two-dimensional calculations have been

performed, one in which the initial temperature and velocity profiles are uniform in the transverse direction and a second in which the initial profiles are nonuniform. A characteristic feature of the temperature profiles is that initially uniform profiles develop overshoots at the walls and initially nonuniform profiles tend to flatten; the latter effect is particularly significant and is primarily attributable to the joule heating that occurs at the electrode-insulator junctions. These results are shown in Figs. 1 and 2 (Appendix I). The differences in the electric current paths are shown in Figs. 1c and 2c (resulting from initially uniform gas dynamic profiles), and Figs. 1d and 2d (resulting from initially nonuniform profiles). . Two significant characteristics of the electric current paths are found to be (1) appreciable eddy current flow both upstream and downstream of the powered section - in fact, the length of the current carrying zone is on the order of twice the length of the powered section, and (2) the current path between the ends of the powered section is directed approximately straight across the channel if the transverse temperature profile is nearly uniform, but it follows an irregular path (j_x is comparable in magnitude to j_y) if the temperature profile is nonuniform. In all the test cases that were computed for these two accelerators, it was found that the wall temperature at the downstream electrode-insulator junctions is a highly nonlinear function of the electrode current density at the points, which in fact determined the downstream values of j_n that were specified in the analysis.

The typical differences in downstream values between variables calculated from (1) quasi-one-dimensional analyses and (2) transverse averages of two-dimensional analyses initiated with nonuniform profiles are as follows:

p	9 percent
u	2 percent
T	7 percent
H	3 percent

Calculations have been performed for flow through Accelerator C to test the capability of the theory to predict results which will compare favorably with available experimental data. This objective is tested by comparing theoretical predictions with impact pressure measurements made at the channel exit. Since the initial profiles entering the channel were not measured, an empirical method is employed in choosing the profiles that gives agreement with the experimental impact pressure measured in the B-field plane for a given run. The details of the method are described in Ref. 5. It contains the premise that since the describing equations are inviscid the initial profiles should include nonuniformity to compensate for the effects of boundary-layer buildup.

The salient feature of the technique is the hypothesis that the appropriate amount of initial nonuniformity is that which results in $\frac{\partial u}{\partial z}\Big|_{wall} = 0$ in the accelerator exit region. In order to complete the specification of the initial-boundary value problem it is necessary to prescribe the applied current on the electrode walls. In the analyses for Accelerators A and B it is stipulated that $j_n(x)$ is the same on the cathode and anode walls. This is done in view of the fact that the segmented electrodes in those channels are small in length compared to channel height. The postulated boundary condition that j_n is a specified function of x would seem appropriate since this implies infinitely fine segmentation. This same assumption was used in an initial attempt to calculate the flow through Accelerator C even though this device has large electrodes. The solutions for the gas dynamic variables were almost symmetric about the centerline (Fig. 3) in contrast to experimental results (impact pressures measured in the exit region) for this channel (Fig. 3c), which demonstrates the necessity of including current concentration. Subsequent calculations have been made in which the specified j_n distribution on the walls has been chosen to cause the current to flow in a direction generally from the anode downstream corner to the cathode upstream corner, which is known to occur from both theoretical considerations and physical observations. The results for impact pressures (Fig. 3c) do indicate asymmetry, and furthermore, the larger theoretical values of impact pressures occur along the anode wall in accord with experiment. However, although the average impact pressures show favorable agreement between theory and experiment, the theoretical results do not display nearly as much nonuniformity as the measured quantities. The current paths in the powered portion of the accelerator (Fig. 3d) naturally reflect the assumed boundary constraints on $(j_n)_{wall}$, but in the entrance and exit regions the fringing that occurs is relatively independent of the assumption that is made of current distribution along the walls. These theoretical results were obtained by assuming that the magnitude of electric current applied to the channel was that which had resulted experimentally when the applied voltage equaled four times the induced voltage. Another attempt to compare theory and experiment was performed at a higher power level (applied voltage equal to six times induced voltage) but resulted in numerical instabilities that could not be resolved as a consequence of the temperature becoming unbounded on the anode wall.

3.2 HALL GENERATOR

The one- and two-dimensional Hall generator programs have been used to compute a case simulating a design point of the LORHO 20-MW

generator described in Ref. 12. The values of the gas dynamic state upstream of the magnetic field, terminal voltage, and seed rate are the same for both methods. It is found that the two-dimensional solution has higher values of pressure, temperature, and axial current (Fig. 4). Since the potential difference between the terminals is the same for both analyses the higher current implies a greater generation of power (greater by 16 percent for the case selected). The change in pressure across the channel is also found to be 16 percent. The electrical current paths and Hall voltage distribution are shown in Figs. 4c and d, respectively. The current paths are the resultant of the generated axial current and the transverse current which is short-circuited through the external circuitry. The values of Hall voltage obtained from one- and two-dimensional approximations to the describing equations compare closely (Fig. 4d), differing by 3 percent at most.

SECTION IV
CONCLUSIONS

The comparison of the averaged two-dimensional with the quasi-one-dimensional calculations of gas dynamic variables shown in Figs. 1b and 2b indicates that the closeness of agreement depends upon whether the gas influx to the channel in question is uniform (using compression heated flow as a gas source, for example) or nonuniform (such as that emanating from an electric arc heater). In the former case the comparison is quite close, which would seem to indicate that in such an application the quasi-one-dimensional solution could be used for the purpose of carrying out design calculations. In the latter case (initial nonuniform profiles) the differences can be as much as 10 percent, which would tend to indicate a greater need to use two-dimensional solutions for performance predictions in these applications. In both instances there is a dissipation of applied electric power because of current fringing in the end regions, the effective current carrying zone being almost twice as long as the length of the electrode section. Initially, nonuniform profiles result in additional power dissipation in the electrode region as is shown by the existence of appreciable local Hall currents (on the order of the applied Faraday current) even though the average Hall current is constrained to be zero. In any case if the flow at the accelerator exit is to be used as a uniform test medium, a two-dimensional solution will have to be carried out for the particular inlet condition considered. The two-dimensional nature of the flow can be severely aggravated as a result of being accelerated by MHD forces.

The comparison of theory with experiment in the one case tested reveals that the predicted impact pressures are greater on the anode wall than on the cathode wall, in accord with measurements, and the average values are comparable. However, more refined criteria for specifying the nonuniformity in the initial profiles is needed since there is substantial disagreement between theory and experiment in the amount of nonuniformity in the exit region.

The comparison of one- and two-dimensional solutions for flow through a linear Hall generator operated in a two-terminal mode shows that if the upstream gas dynamic state, seed rate, and terminal voltage are matched, the generated power is larger in the two-dimensional case (16 percent in the test case analyzed). The two-dimensional analysis gives the end effects caused by (1) the fringing magnetic field and (2) the conduction of the electrical current through the terminals into the flowing gas. Although a small difference in generated power was experienced because of the end effects in the case considered (16 percent as previously noted) each generator design should be investigated. A more important aspect of the two-dimensional analysis is the calculation of the pressure gradient transverse to the flow. This gradient can have adverse effects on the boundary layer in the channel.

It would not have been possible to obtain any of the two-dimensional solutions presented in this report without using the direct method of Ref. 4 to solve the finite difference relations. The simplicity, stability, and accuracy of the method is such that it is recommended in general to solve systems of second-order finite difference equations in preference to other methods that have been proposed in the literature.

REFERENCES

1. Sutton, G. W. and Sherman, A. Engineering Magnetohydrodynamics. McGraw-Hill, New York, 1965.

2. Snyder, W. T. and Maus, J. R. "Internal MHD Channel Flows Including Hall Effect and Variable Fluid Properties." AEDC-TR-70-26 (AD701386), February 1970.

3. Argyropoulos, G. S. and Demetriades, S. T. "Current Distribution in Crossed-Field Accelerators (Part IV, Project Summary and Application)." AEDC-TR-71-91 (AD722443), April 1971.

4. Schechter, S. "Quasi-Tridiagonal Matrices and Type-Insensitive Difference Equations." Quarterly of Applied Mathematics, Vol. 18, 1960, pp. 285-295.

5. Johnson, P. W. "Two-Dimensional Flow Calculations in the Magnetic Field Plane for Linear MHD Channels." AEDC-TR-71-20 (AD880611), February 1971.

6. Neel, C. A. and Lewis, C. H. "Interpolations of Imperfect Air Thermodynamic Data. I. At Constant Entropy." AEDC-TDR-64-183 (AD605471), September 1964.

7. Brahinsky, H. S. and Neel, C. A. "Tables of Equilibrium Thermodynamic Properties of Nitrogen." AEDC-TR-69-126 (AD693134), August 1969.

8. Garrison, G. W. "Electrical Conductivity of a Seeded Nitrogen Plasma." AIAA Journal, Vol. 6, No. 7, July 1968, pp. 1264-1270.

9. Lin, S. C., Resler, E. L., and Kantrowitz, A. "Electrical Conductivity of Highly Ionized Argon Produced by Shock Waves." Journal of Applied Physics, Vol. 26, No. 1, January 1955, p. 95.

10. Demetriades, S. T. and Argyropoulos, G. S. "Ohm's Law in Multicomponent Nonisothermal Plasma with Temperature and Pressure Gradients." The Physics of Fluids, Vol. 9, No. 11, November 1966, p. 2136.

11. Norman, W. and Siler, L. G. "Experiments on a Shock Tunnel Augmented by a Magnetohydrodynamic Nozzle Accelerator." AEDC-TR-68-232 (AD844665), December 1968.

12. Windmueller, A. K., Wright, L. E., and Luchuk, W. "Operating Experience with the AEDC 20-Megawatt Magnetohydrodynamic Hall Generator." AEDC-TR-70-212 (AD874831), October 1970.

APPENDIXES

I. ILLUSTRATIONS
II. CONTINUITY OF MASS AND ELECTRIC CURRENT (SOURCE FLOW)
III. TRANSFORMATION OF EQUATIONS OF MOTION
IV. THERMODYNAMIC FUNCTIONS
V. ELECTRIC CURRENT DENSITY IN FARADAY CHANNELS
VI. ELECTRIC POTENTIAL IN HALL CHANNELS
VII. DIRECT METHOD OF SOLUTION OF FINITE DIFFERENCE EQUATIONS
VIII. TABLES

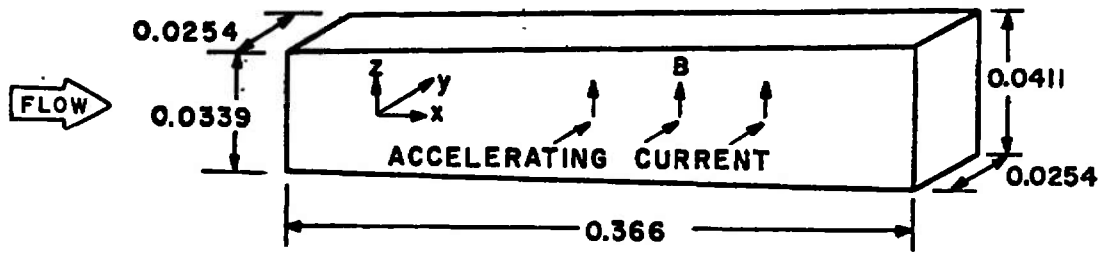

NOTE: ALL DIMENSIONS IN METERS

OPERATING GAS ~ NITROGEN

SEED ~ POTASSIUM (0.50 % by Weight)

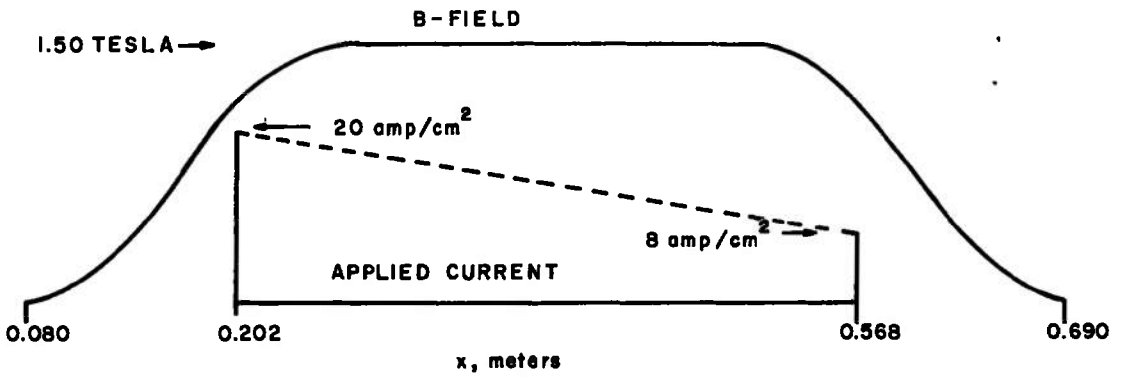

a. Geometry and Applied Fields

Fig. 1 MHD Flow Field in Accelerator A

AVERAGE DOWNSTREAM VALUES

(x = 0.82 meters)

p/p_∞	u_{avg} m/sec	T_{avg} °K	$H_{avg} \times 10^{-6}$ m²/sec²
QUASI-ONE-DIMENSIONAL			
0.207	2978	3007	8.07
TWO-DIMENSIONAL UNIFORM INITIAL PROFILES			
0.212	2944	3047	8.02
NONUNIFORM INITIAL PROFILES			
0.226	2936	3228	8.23

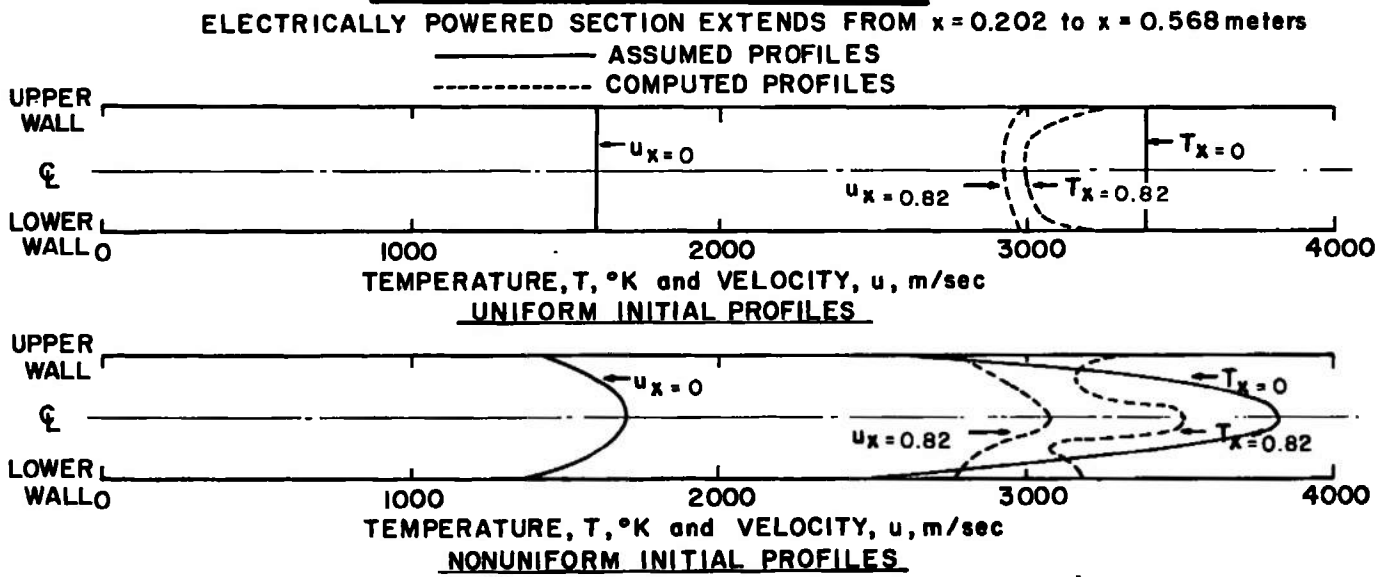

b. Velocity and Temperature; Uniform versus Nonuniform Initial Profiles

Fig. 1 Continued

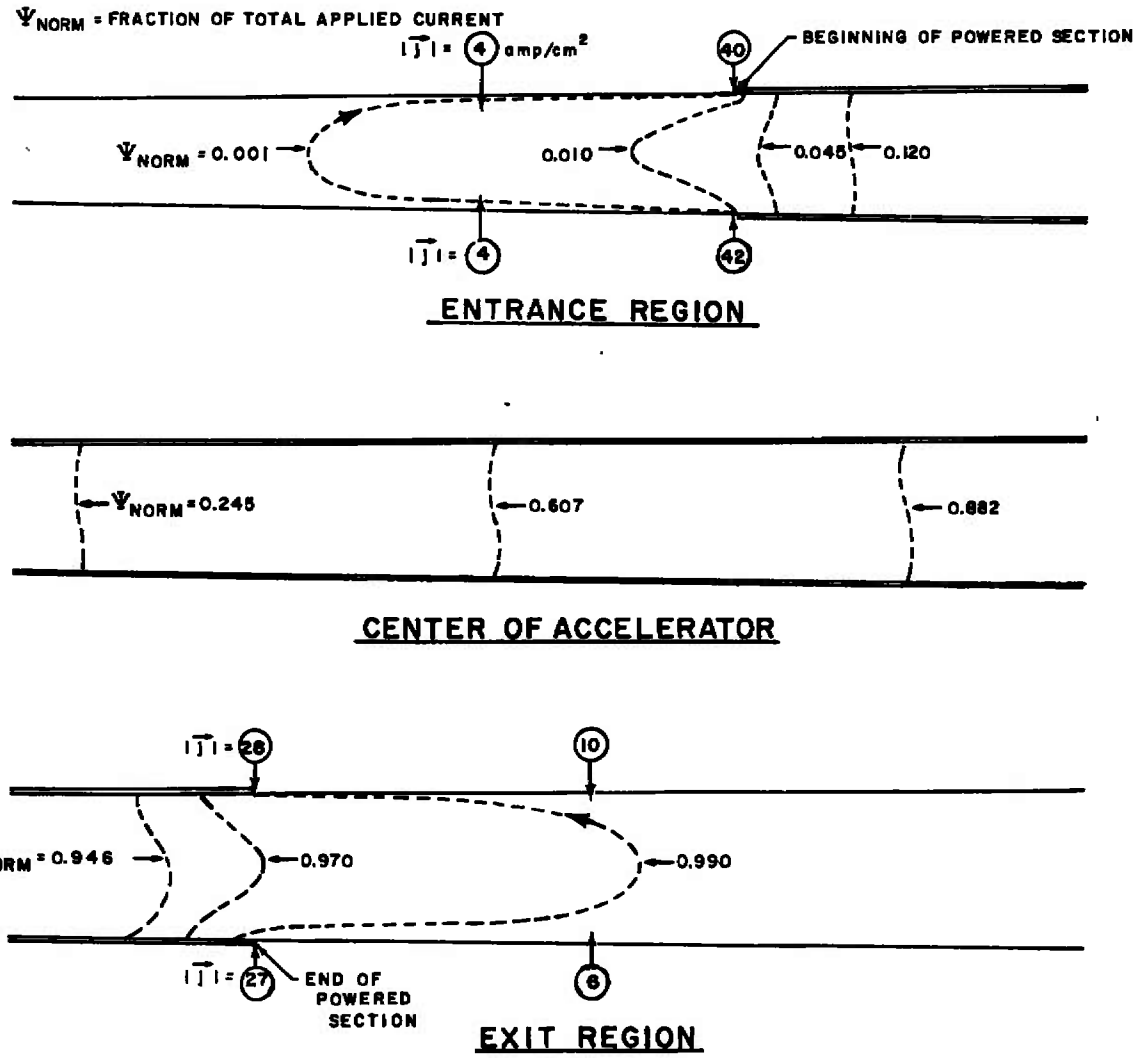

c. Current Density; Uniform Initial Profiles
Fig. 1 Continued

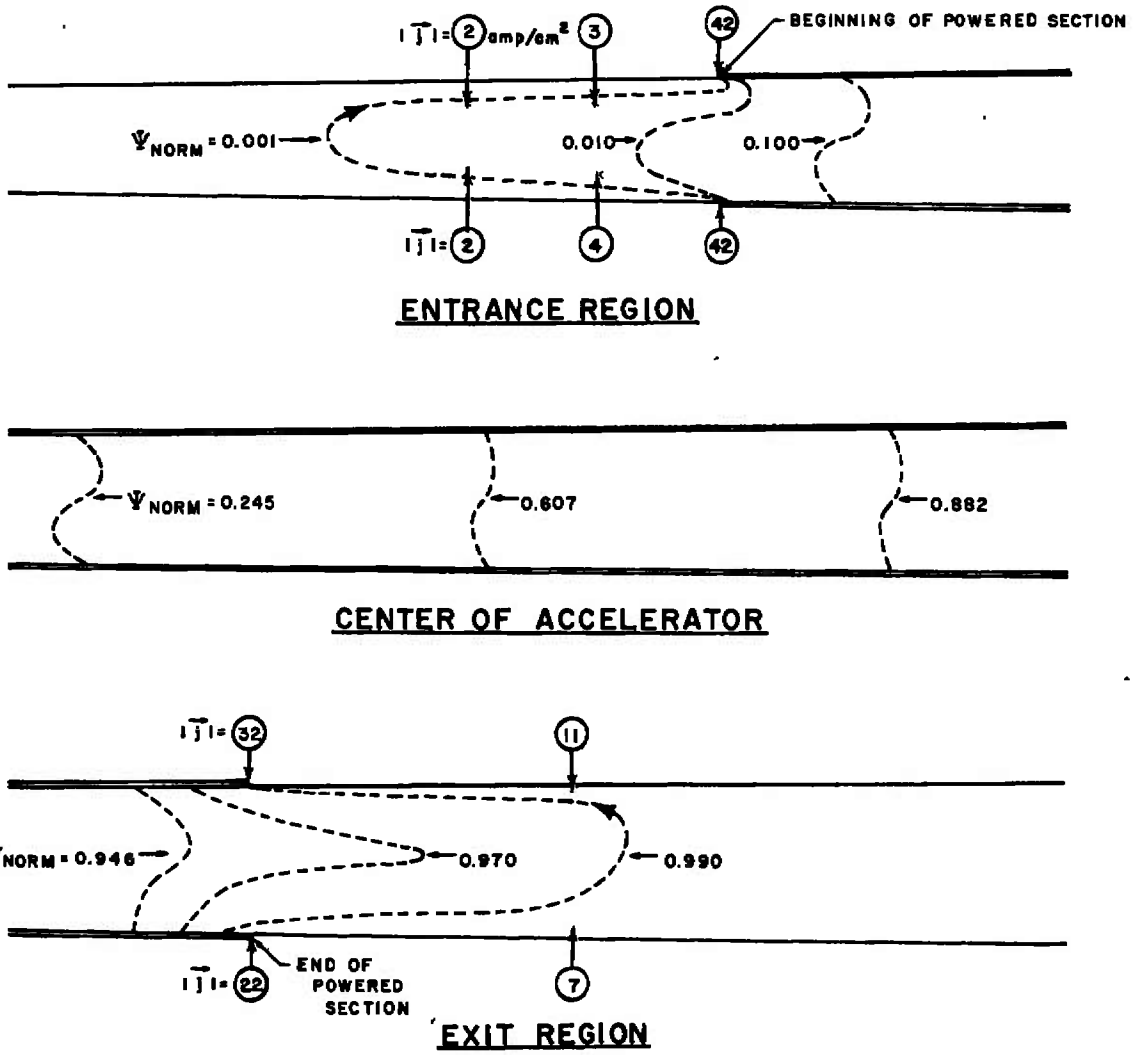

d. Current Density; Nonuniform Initial Profiles
Fig. 1 Concluded

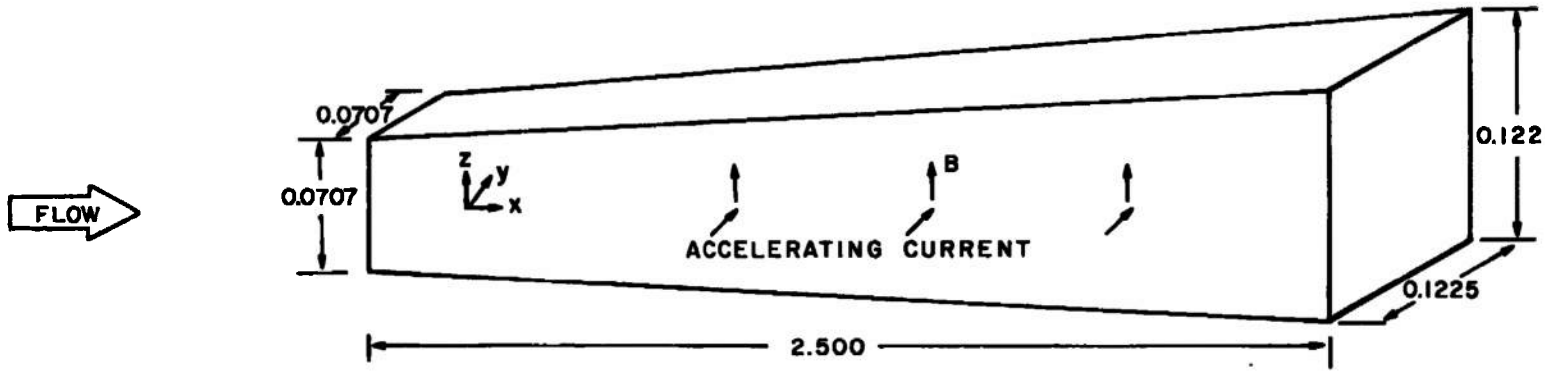

NOTE: ALL DIMENSIONS IN METERS

OPERATING GAS ~ AIR

SEED ~ POTASSIUM (0.50 % by Weight)

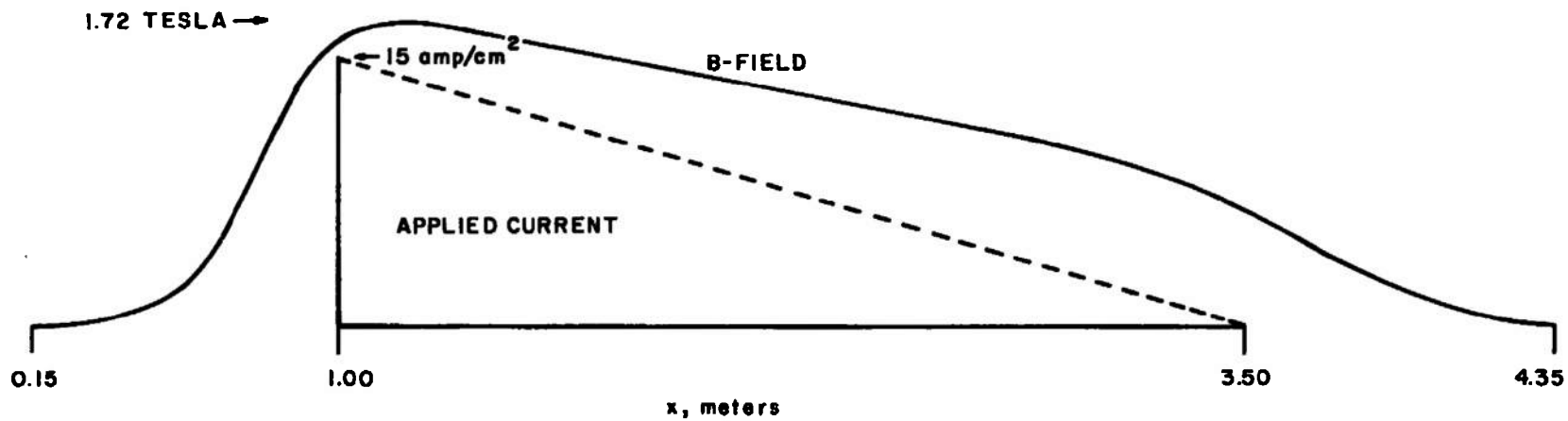

a. Geometry and Applied Fields

Fig. 2 MHD Flow Field in Accelerator B

AEDC-TR-71-181

AVERAGE DOWNSTREAM VALUES
(x = 4.48 meters)

p/p_∞	u_{avg} m/sec	T_{avg} °K	$H_{avg} \times 10^{-6}$ m^2/sec^2
QUASI - ONE - DIMENSIONAL			
0.047	6394	2850	24.9
TWO - DIMENSIONAL			
UNIFORM INITIAL PROFILES			
0.048	6352	2895	24.8
NONUNIFORM INITIAL PROFILES			
0.051	6350	2999	25.4

ELECTRICALLY POWERED SECTION EXTENDS FROM x = 1.0 to x = 3.5 meters

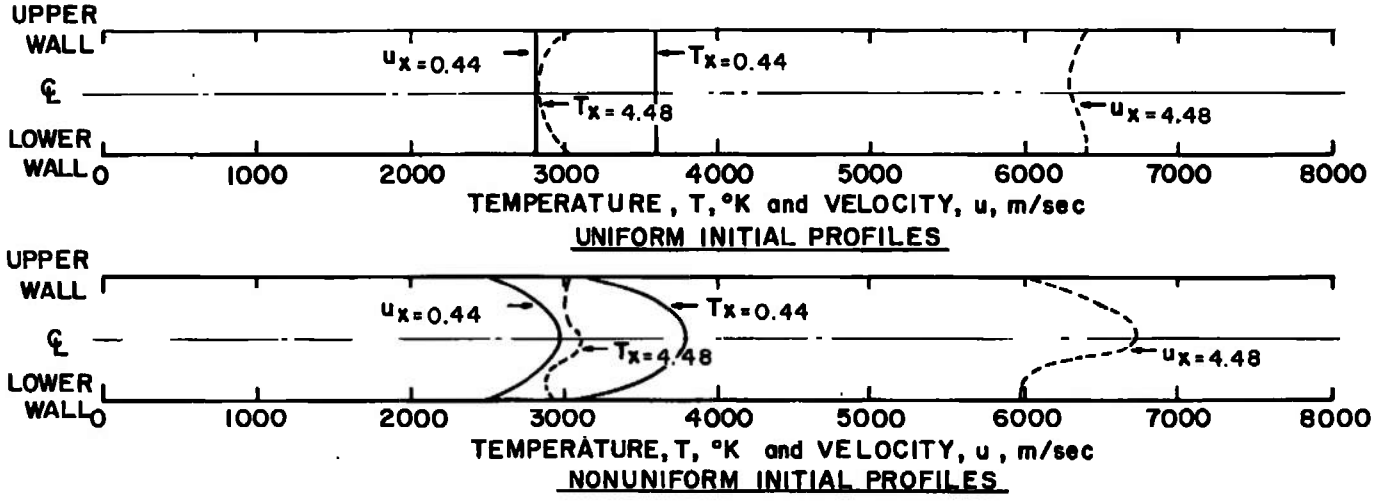

b. Velocity and Temperature; Uniform versus Nonuniform Initial Profiles
Fig. 2 Continued

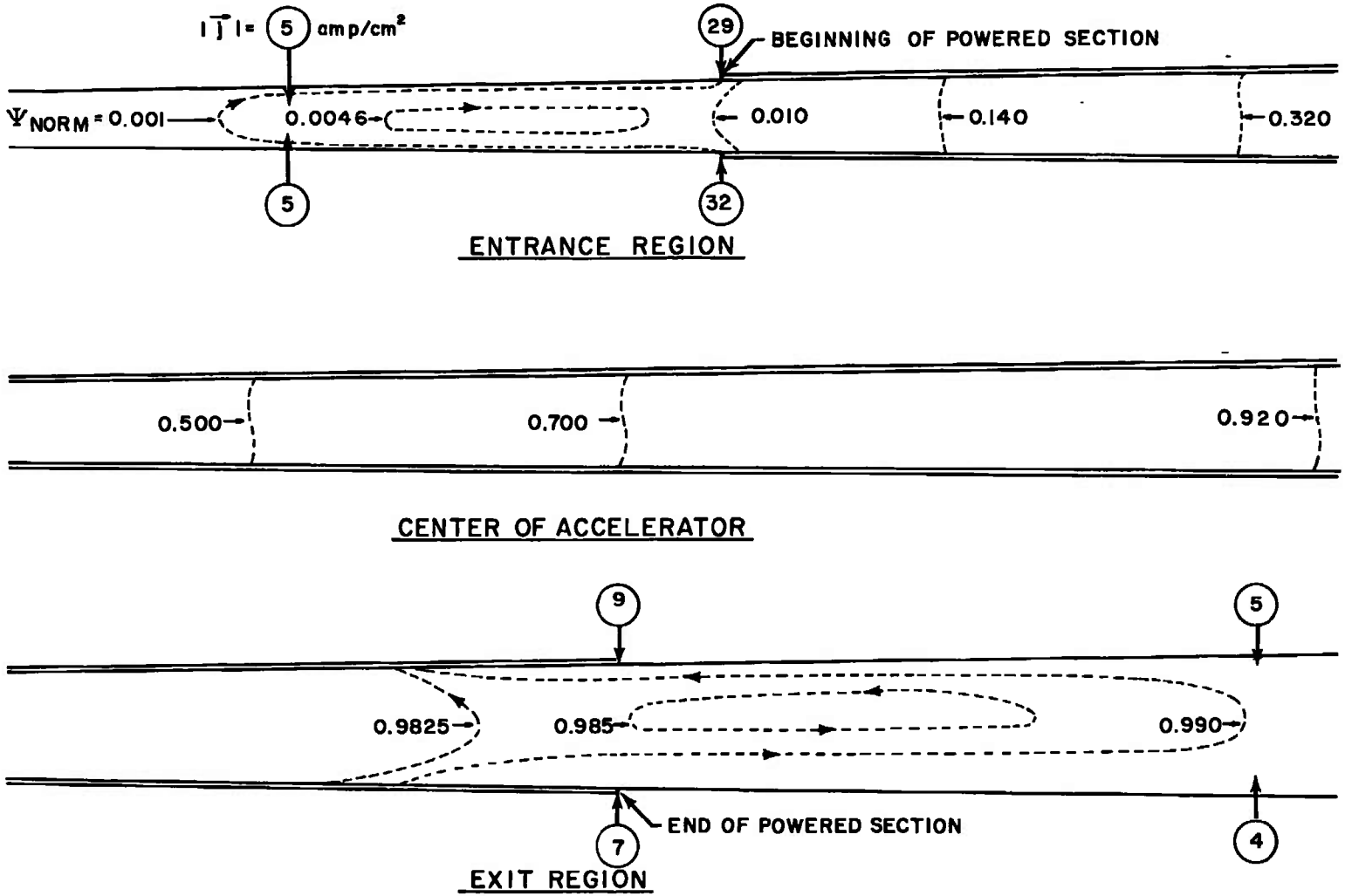

c. Current Density; Uniform Initial Profiles
Fig. 2 Continued

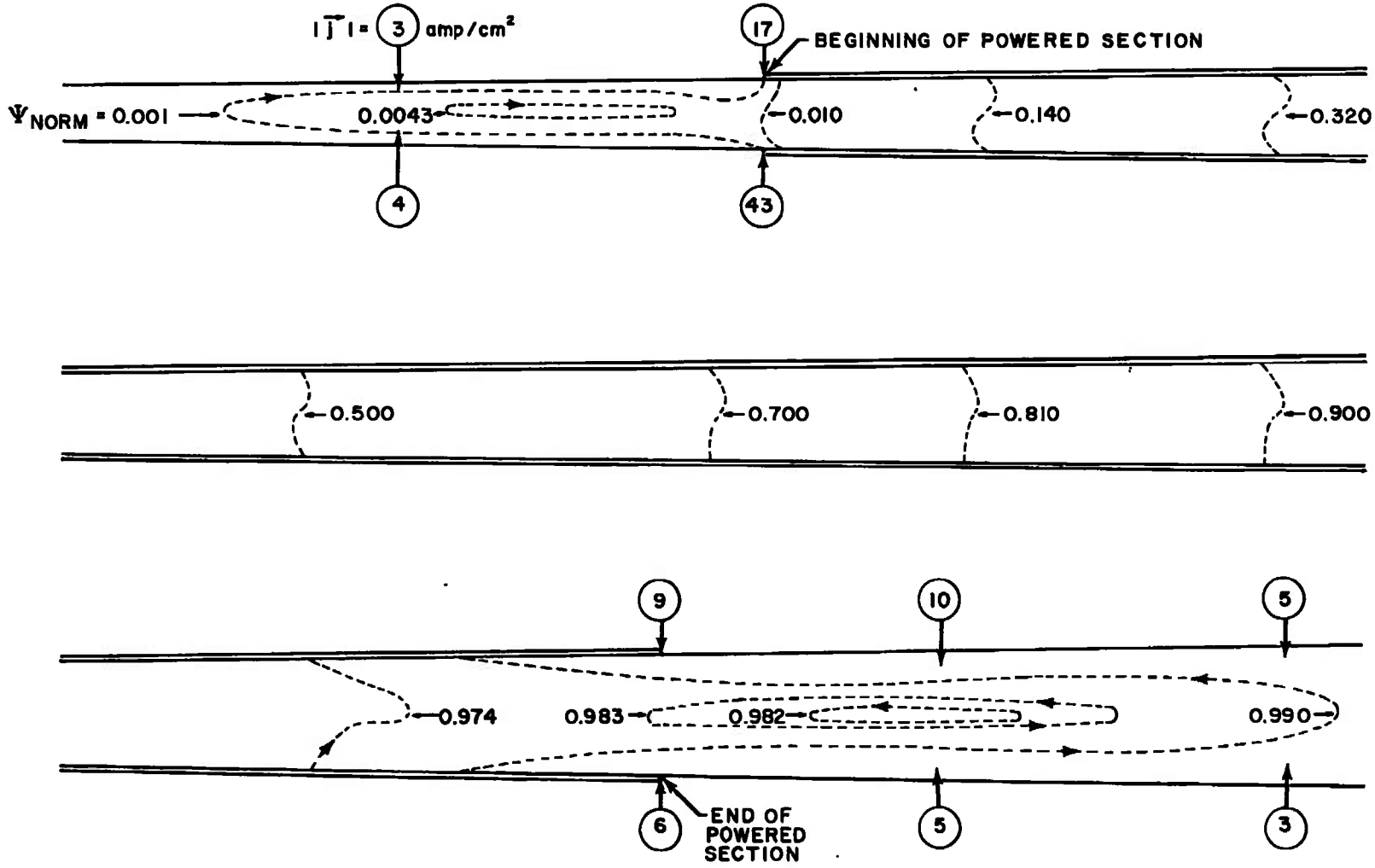

d. Current Density; Nonuniform Initial Profiles

Fig. 2 Concluded

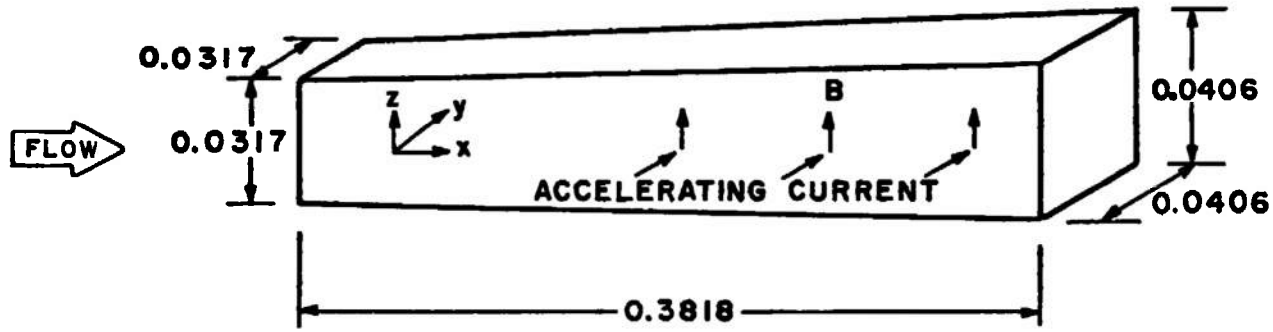

NOTE: ALL DIMENSIONS IN METERS

OPERATING GAS ~ AIR

SEED ~ POTASSIUM (0.20 % by Weight)

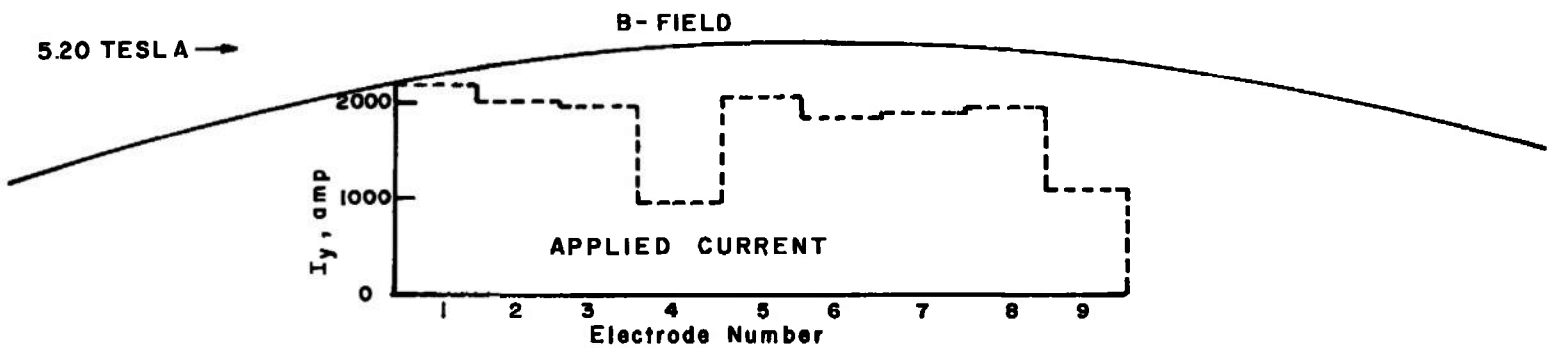

a. Geometry and Applied Fields

Fig. 3 MHD Flow Field in Accelerator C

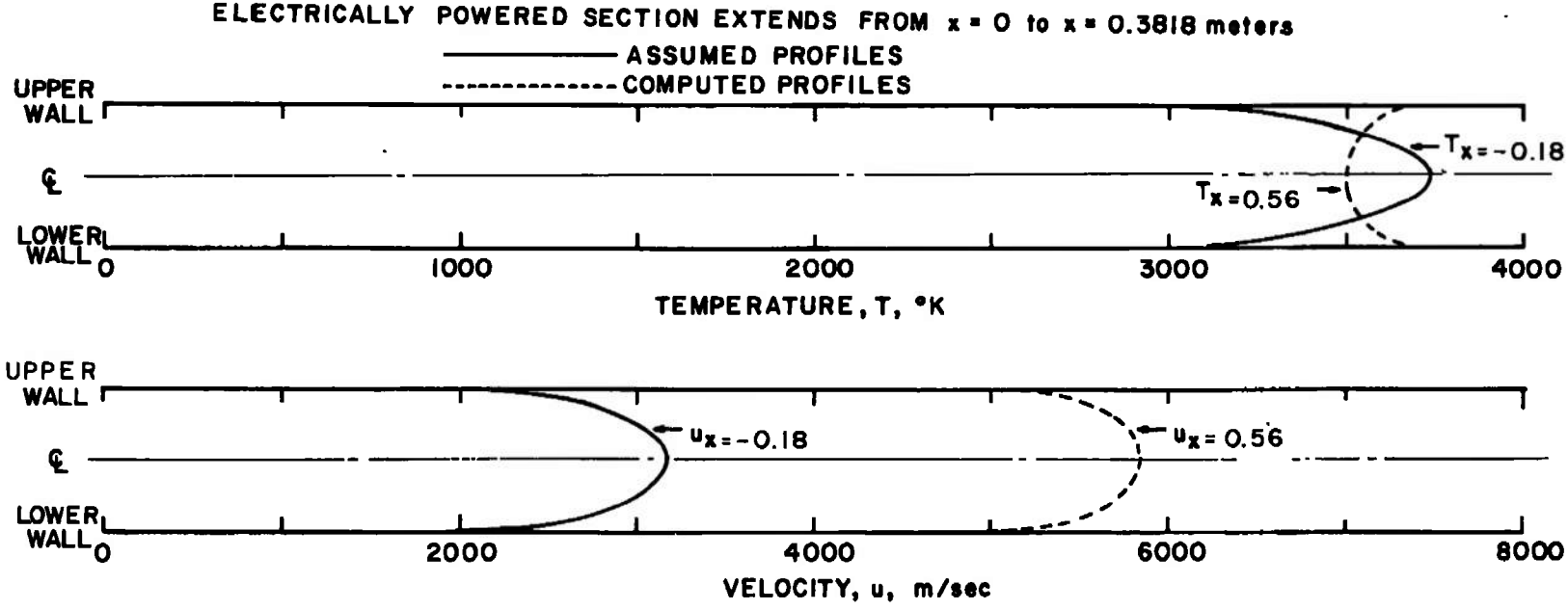

b. Velocity and Temperature without Finite Electrode Segmentation
Fig. 3 Continued

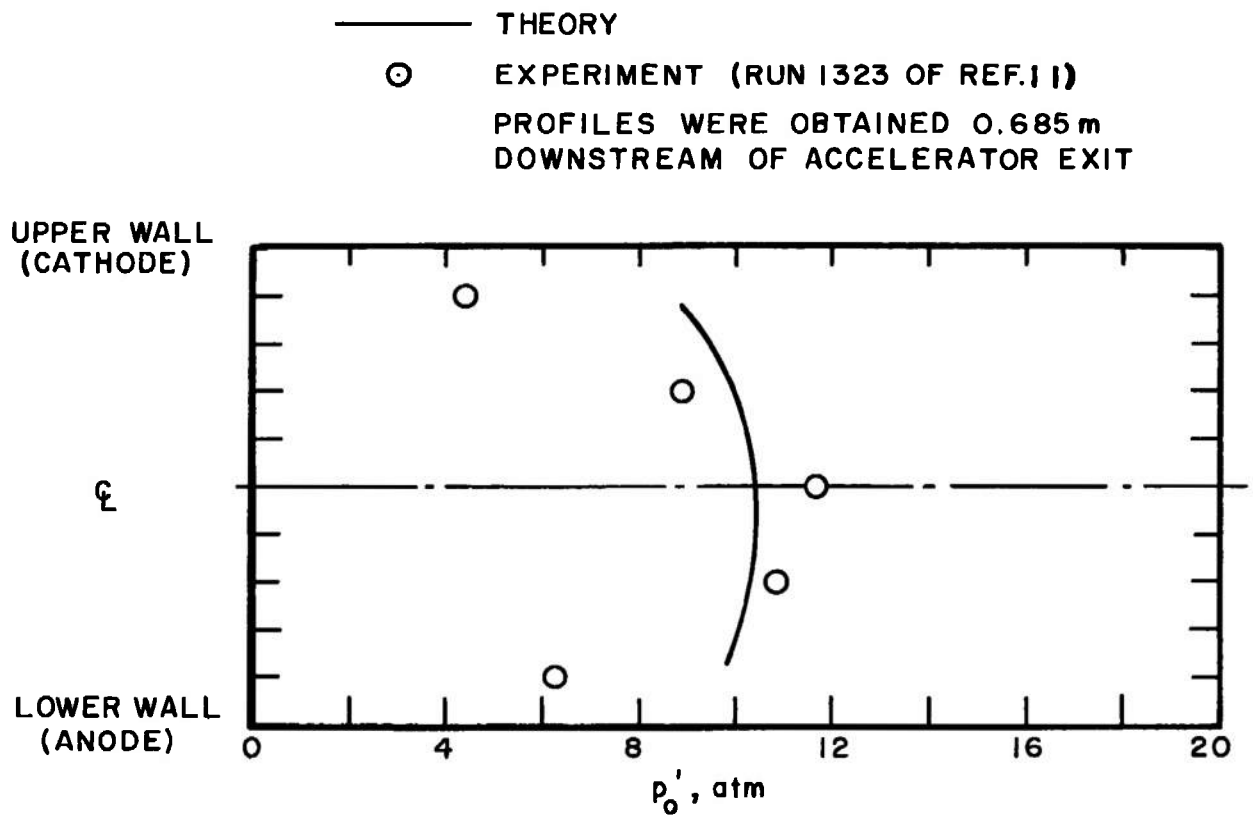

c. Impact Pressures with Finite Electrode Segmentation

Fig. 3 Continued

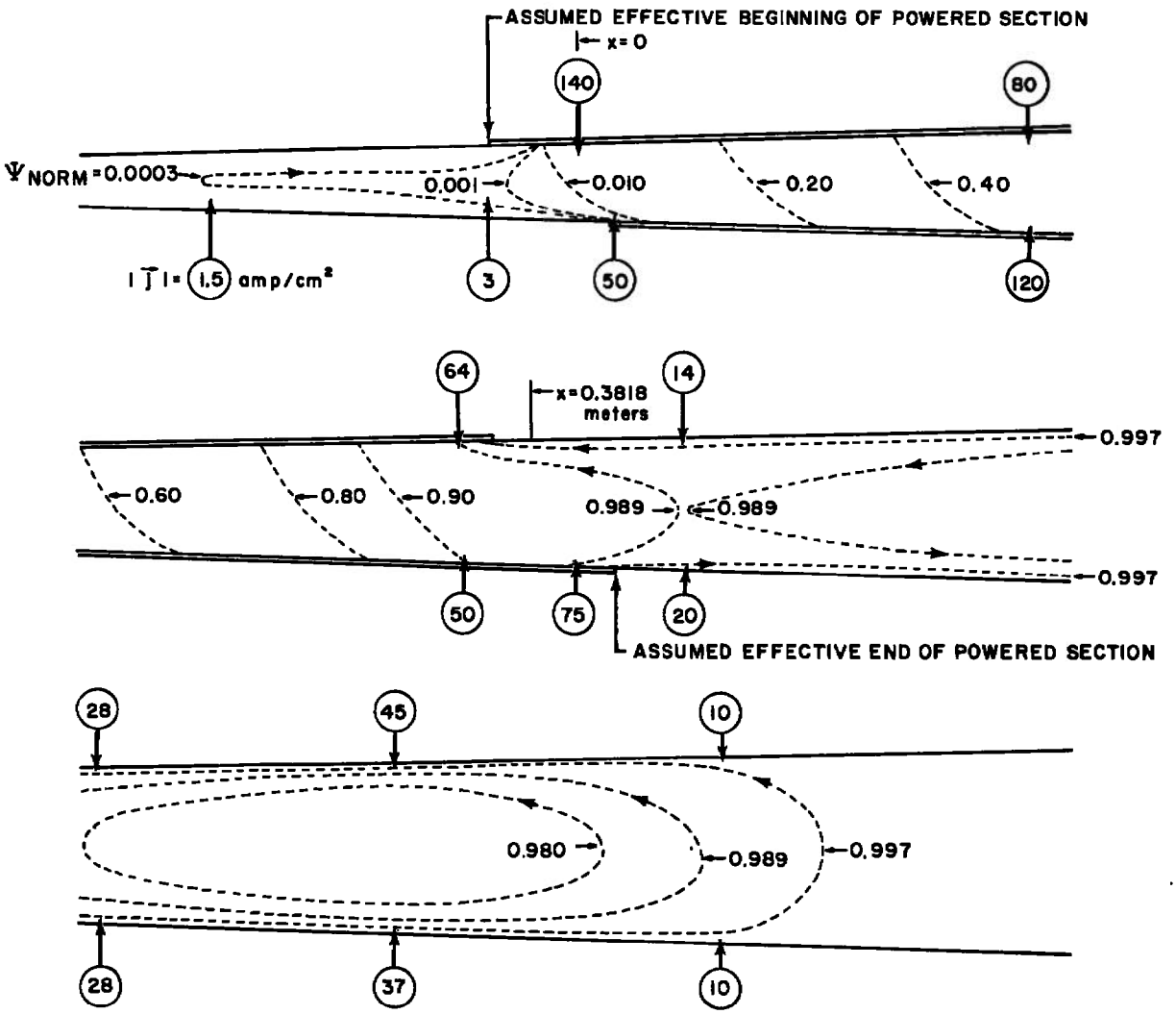

d. Current Density
Fig. 3 Concluded

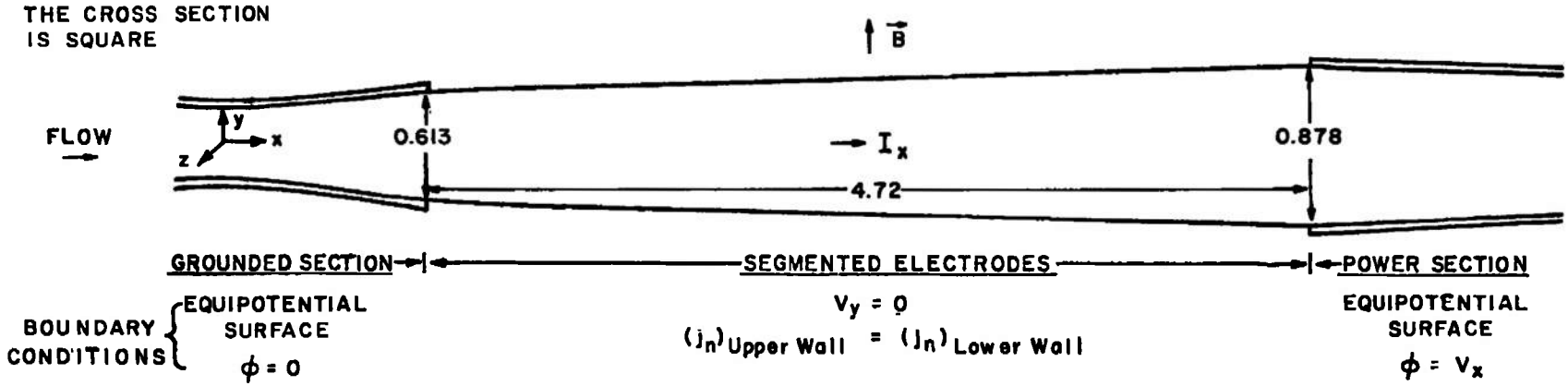

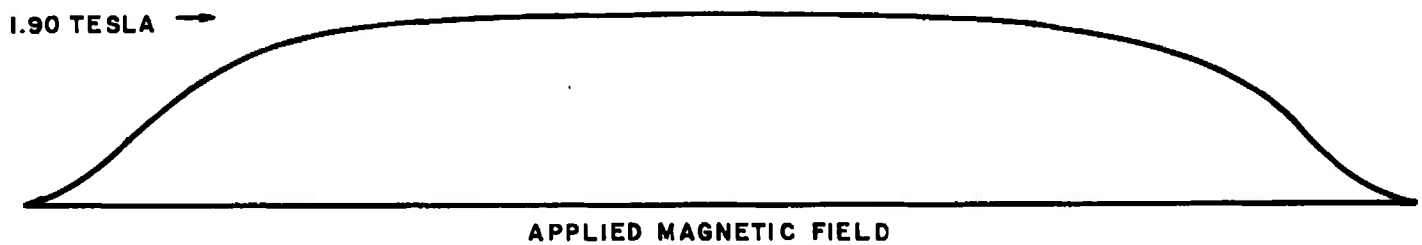

a. Geometry and Applied Fields

Fig. 4 MHD Flow Field in Hall Generator

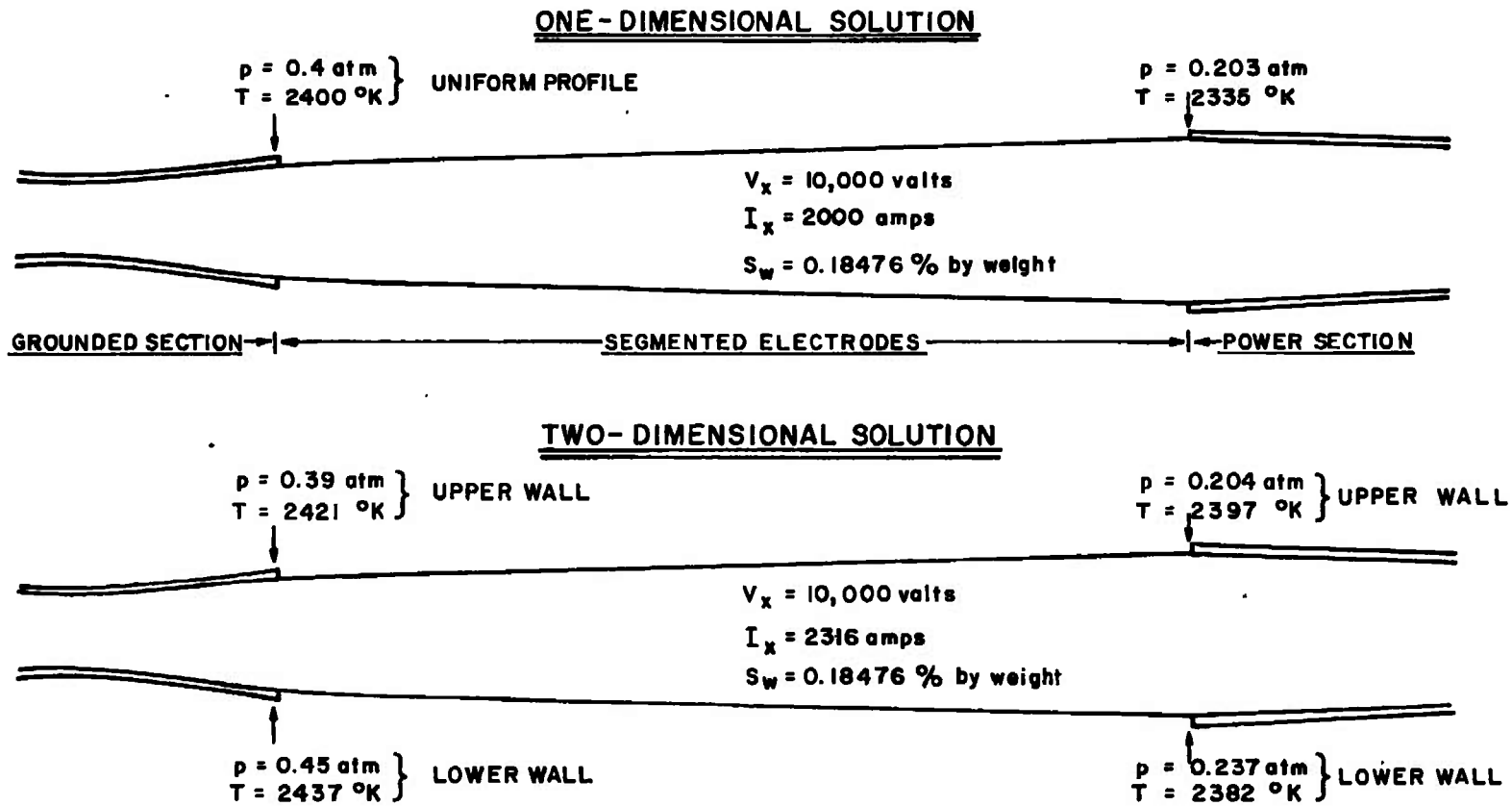

NOTE: GAS DYNAMIC STATE UPSTREAM OF THE MAGNETIC FIELD IS THE SAME FOR BOTH SOLUTIONS

b. One-Dimensional versus Two-Dimensional Solutions
Fig. 4 Continued

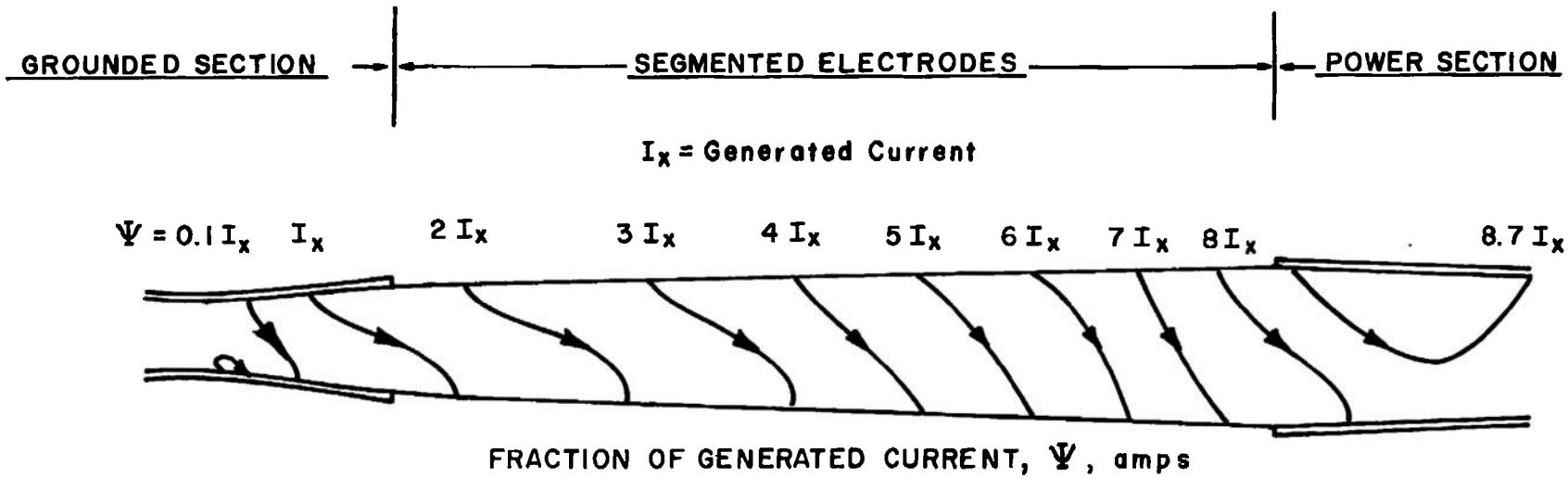

c. Electric Current Paths
Fig. 4 Continued

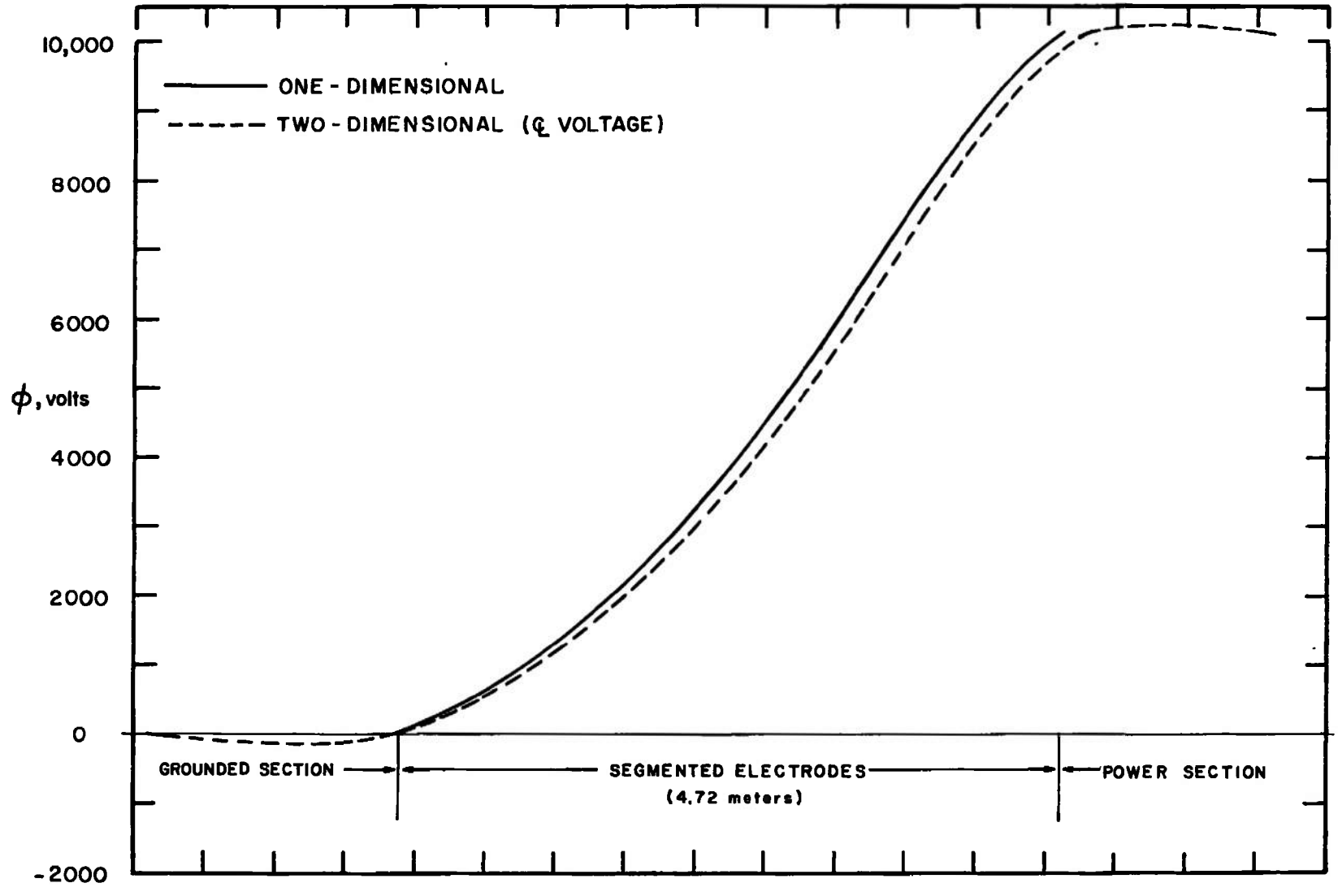

d. Hall Voltage
Fig. 4 Concluded

APPENDIX II
CONTINUITY OF MASS AND ELECTRIC CURRENT (SOURCE FLOW)

The usual forms in which the mass and electric current conservation equations are given, $\nabla \cdot \rho\vec{V} = 0$ and $\nabla \cdot \vec{j} = 0$, are applicable to plane or three-dimensional flows. However, it is incorrect to apply these formulas to the flow model analyzed in this report because the flow is quasi-two-dimensional in the sense described below.

It is intended that the analysis should have the capability of computing flows through channels with divergence of both pairs of sidewalls (the B-field as well as E-field walls) while at the same time expressing the equations of motion as functions of only two spatial coordinates (x and y). In order to accomplish this it is assumed:

1. The x and y components of velocity and current density are functions only of x and y
2. The ratio of the z and x components of velocity and current density satisfy

$$\frac{w}{u} = \frac{z}{W}\frac{dW}{dx}$$

and

$$\frac{j_z}{j_x} = \frac{z}{W}\frac{dW}{dx}$$

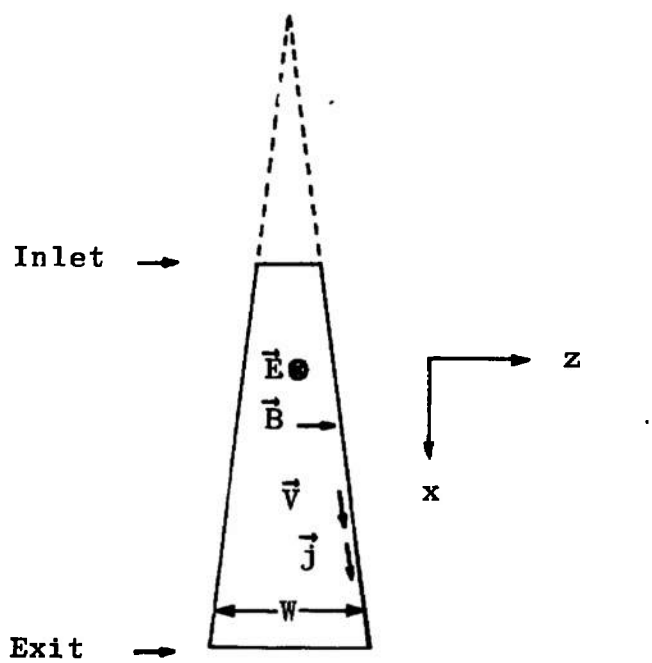

This latter assumption states that the slope of the streamline projection in the x-z plane is a linear function of the z coordinate.

Let $\vec{F} = [F_x, F_y, F_z]$ represent either of the two solenoidal vectors, $\rho\vec{V}$ or $\vec{j}$. The combination of the above assumptions with $\nabla \cdot \vec{F}(x, y, z) = 0$ yields

$$\nabla\cdot\vec{F}(x,y,z) = \frac{\partial}{\partial x} F_x(x,y) + \frac{\partial}{\partial y} F_y(x,y) + \frac{\partial}{\partial z}\left[F_x(x,y)\ \frac{z}{W}\frac{dW}{dx}\right]$$

$$= \frac{\partial}{\partial x} F_x + \frac{\partial}{\partial y} F_y + \frac{F_x}{W}\frac{dW}{dx}$$

$$= \frac{1}{W}\frac{\partial}{\partial x} WF_x + \frac{\partial}{\partial y} F_y$$

$$= \frac{1}{W}\left(\frac{\partial}{\partial x} WF_x + \frac{\partial}{\partial y} WF_y\right)$$

$$= 0$$

The conclusions are

$$\frac{\partial}{\partial x} W\rho u + \frac{\partial}{\partial y} W\rho v = 0 \qquad \text{(II-1)}$$

and

$$\frac{\partial}{\partial x} Wj_x + \frac{\partial}{\partial y} Wj_y = 0 \qquad \text{(II-2)}$$

Equation (II-1) suggests the definition of a (normalized) mass stream function which satisfies

$$\frac{\partial \psi}{\partial x} = -\frac{2W}{\dot{m}}\rho v$$

$$\frac{\partial \psi}{\partial y} = \frac{2W}{\dot{m}}\rho u \qquad \text{(II-3)}$$

where the normalization has been chosen such that $\psi = 1$ on the upper wall and $\psi = -1$ on the lower wall. Equation (II-2) suggests the definition of an electric current stream function which satisfies

$$\frac{\partial \Psi(x,y)}{\partial x} = -Wj_y$$

$$\frac{\partial \Psi(x,y)}{\partial y} = Wj_x \qquad \text{(II-4)}$$

The solution of the describing equations is performed using von Mises coordinates; this requires Ψ to be expressed as a function of (x, ψ) as follows

$$\frac{\partial \Psi(x,\psi)}{\partial x} = -\left[\frac{\partial x}{\partial s}(s,n)\right]^{-1} Wj_n$$

$$\frac{\partial \Psi(x,\psi)}{\partial \psi} = \left[\frac{\partial \psi}{\partial y}(x,y)\right]^{-1} Wj_x$$

where (s, n) are orthonormal coordinates measured tangential and normal to fluid particle paths.

APPENDIX III
TRANSFORMATION OF EQUATIONS OF MOTION

The gas dynamic equations are solved after rearranging the steady-state form of the conservation equations for

Mass (Source Flow)

$$\nabla \cdot W\rho\vec{V} = 0 \tag{III-1}$$

Momentum

$$\rho \frac{D\vec{V}}{Dt} + \nabla p = \vec{j}x\vec{B} \tag{III-2}$$

Energy

$$\rho \frac{DH}{Dt} = \vec{E}\cdot\vec{j} \tag{III-3}$$

into a system of differential equations where the dependent variables are $q(x, \psi)$, $p(x, \psi)$, $T(x, \psi)$ in the accelerator analysis, and $q(x, \psi)$, $p(x, \psi)$, $H(x, \psi)$ in the generator analysis. These variables were selected because they are of special importance, and because the thermodynamic functions are expressed as functions of p and T in the accelerator analysis, and p and h in the generator analysis.

The equation for q is obtained by combining the components of the momentum Eq. (III-2) to yield (in von Mises coordinates)

$$\rho u \frac{\partial}{\partial x}\frac{q^2}{2} + u \frac{\partial p}{\partial x} = [VjB] \tag{III-4}$$

The assumption that $\vec{B}$ has a component in the z-direction only implies

$$[VjB] = \left(\frac{\partial x}{\partial s}\right)^{-1} u j_n B \tag{III-5}$$

where

$$j_n = \frac{\partial x}{\partial s} j_y - \frac{\partial y}{\partial s} j_x$$

$$\frac{\partial x}{\partial s} = \left\{1 + \left[\frac{\partial y}{\partial x}(x, \psi)\right]^2\right\}^{-1/2}$$

$$\frac{\partial y}{\partial s} = \frac{\frac{\partial y}{\partial x}}{\left\{1 + \left(\frac{\partial y}{\partial x}\right)^2\right\}^{1/2}}$$

and $\frac{\partial y}{\partial x}(x,\psi)$ is given by Eq. (4).

The result is

$$\frac{\partial q}{\partial x}(x,\psi) = (\rho q)^{-1}\left[\left(\frac{\partial x}{\partial s}\right)^{-1} j_n B - \frac{\partial p}{\partial x}\right]$$

in which form the solution is obtained using a Runge-Kutta method, and the pressure gradient that appears on the right-hand side is evaluated below.

The pressure is computed on two levels of approximation. The first level of approximation consists of solving a system of streamline differential equations for pressure. This is followed by a second level of approximation in which the pressure is recomputed by integrating the transverse momentum equation in the y direction. These approximations are obtained from the following sequence of calculations: conservation of mass is expressed in integral form; this integral relationship is differentiated in the streamline direction; by invoking an equation of state, and momentum and energy conservation, a system of integral equations for streamline pressure gradient is obtained; these integral equations are then formally inverted to obtain the required formula for pressure prediction to be performed in an explicit manner.

The detailed derivation of the formula for $\frac{\partial}{\partial x} p_i(x, \psi)$, where p_i is the pressure on the ith streamline, begins by differentiating

$$A = W\int_{-\frac{d}{2}}^{\frac{d}{2}} dy \doteq W\int_{-1}^{1}\left(\frac{\partial \psi}{\partial y}\right)^{-1} d\psi = \frac{\dot{m}}{2}\int_{-1}^{1}\left(\frac{\partial x}{\partial s}\rho q\right)^{-1} d\psi$$

to obtain

$$\frac{dA}{dx} = \frac{\dot{m}}{2}\int_{-1}^{1}\frac{\partial}{\partial x}\left(\frac{\partial x}{\partial s}\rho q\right)^{-1} d\psi$$

The next step is to substitute into the previous equation either Eqs. (III-6) to (III-10) in the case of the accelerator analysis.

$$\rho = \rho(p,T) \tag{III-6}$$

$$\frac{\partial \rho}{\partial x} = \frac{\partial \rho}{\partial p}\frac{\partial p}{\partial x} + \frac{\partial \rho}{\partial T}\frac{\partial T}{\partial x} \tag{III-7}$$

$$\frac{\partial T}{\partial x} = \left(\frac{\partial h}{\partial T}\right)^{-1}\left[\left(\frac{1}{\rho} - \frac{\partial h}{\partial p}\right)\frac{\partial p}{\partial x} + \frac{\vec{E}\cdot\vec{j} - [VjB]}{\rho u}\right] \tag{III-8}$$

(Eq. (III-8) follows from Eqs. (8) and (III-4))

$$M^2 = q^2\left[\frac{\partial \rho}{\partial p} + \frac{\partial \rho}{\partial T}\left(1 - \rho\frac{\partial h}{\partial p}\right)\left(\rho\frac{\partial h}{\partial T}\right)^{-1}\right] \tag{III-9}$$

$$F_1 = \left(\frac{\partial h}{\partial T}\right)^{-1}\frac{\partial \rho}{\partial T} \tag{III-10}$$

or Eqs. (III-11) to (III-15) in the case of the generator analysis

$$\rho = \rho(p,h) \tag{III-11}$$

$$\frac{\partial \rho}{\partial x} = \frac{\partial \rho}{\partial p}\frac{\partial p}{\partial x} + \frac{\partial \rho}{\partial h}\frac{\partial h}{\partial x} \tag{III-12}$$

$$\frac{\partial h}{\partial x} = \frac{\vec{E}\cdot\vec{j}}{\rho u} - \frac{\partial}{\partial x}\frac{q^2}{2} \tag{III-13}$$

(Eq. (III-13) follows from Eq. (8))

$$M^2 = \frac{q^2}{RZT}\left[1 - \rho\frac{\partial}{\partial p}(RZT) - \frac{\partial}{\partial h}(RZT)\right] \tag{III-14}$$

$$F_1 = \frac{\partial \rho}{\partial h} \tag{III-15}$$

In addition both analyses use Eq. (16), which implies

$$\vec{E}^*\cdot\vec{j} = \vec{E}\cdot\vec{j} - [VjB]$$

$$= \frac{j_s^2 + j_n^2}{\sigma}$$

and the identity which makes it possible to formally invert the pressure integral equations

$$\frac{\partial}{\partial x} p_j \equiv \frac{\partial}{\partial x} (p_j - p_i) + \frac{\partial}{\partial x} p_i$$

to achieve the result

$$\frac{\partial}{\partial x} p_i = \frac{-\frac{2}{\dot{m}} \frac{dA}{dx} + F_2 - F_3}{\int_{-1}^{1} \left(\frac{\partial x}{\partial s} \rho^2 q^3\right)^{-1} (M^2 - 1)\, d\psi}$$

where

$$F_2 = \int_{-1}^{1} (\rho q)^{-1} \frac{\partial}{\partial x} \left(\frac{\partial x}{\partial s}\right)^{-1} d\psi$$

$$F_3 = \int_{-1}^{1} \left(\frac{\partial x}{\partial s} \rho^2 q^3\right)^{-1} \left\{ (M^2 - 1) \frac{\partial}{\partial x} (p_j - p_i) \right.$$

$$\left. + \left(\frac{\partial x}{\partial s}\right)^{-1} (j_n B + \rho^{-1} q\, \vec{E}^* \cdot \vec{j}\, F_1) \right\} d\psi_j$$

The notation ψ_j used for the dummy variable of integration in the second integral of the numerator means that the quadrature is to be performed with the streamlines labeled with j subscripts. This is done in order to define the meaning of $p_j - p_i$ which occurs in this same integral; thus $p_j - p_i$ means the difference between pressures on the jth and ith streamlines. Formally, this pressure difference can be evaluated from the transverse momentum equation where

$$\rho u \frac{\partial v}{\partial x} + \frac{\partial \psi}{\partial y} \frac{\partial p}{\partial \psi} = - j_x B$$

is integrated in the transverse direction and then differentiated in the axial direction to give

$$\frac{\partial}{\partial x} (p_j - p_i) = B \frac{j_n}{\frac{\partial x}{\partial s}} \Bigg|_i^j - \frac{d}{dx} \frac{B}{W} \Psi \Bigg|_i^j - \frac{\dot{m}}{2} \frac{\partial}{\partial x} \left[W^{-1} \int_i^j \frac{\partial v}{\partial x}\, d\psi \right] \quad \text{(III-16)}$$

and $\frac{\partial v}{\partial x}$ is evaluated from

$$v = \frac{\partial y}{\partial x}\left[1 + \left(\frac{\partial y}{\partial x}\right)^2\right]^{-1/2} q$$

and the streamline slope $\frac{\partial y}{\partial x}$ is obtained from Eq. (4). For channels whose conductor walls are only slightly diverged such as that of Ref. 11, the last term on the right-hand side of Eq. (III-16) ≈ 0.

The second approximation for pressure alluded to above is given by the integral of the radial momentum equation

$$p_j - p_i = \frac{B}{W}(\Psi_i - \Psi_j) - \frac{\dot{m}}{2} W^{-1} \int_i^j \frac{\partial v}{\partial x}\, d\psi$$

The difference of current fluxes on the ith and jth streamlines, $\Psi_i - \Psi_j$, is obtained in the case of Faraday channels by the theory described in Appendix V, and from

$$\Psi_j - \Psi_i = W \int_i^j \left(\frac{\partial \psi}{\partial y}\right)^{-1} j_x\, d\psi$$

for channels in which the describing electric equation is that of an electric potential.

APPENDIX IV
THERMODYNAMIC FUNCTIONS

Expressions for thermodynamic functions of air and nitrogen, respectively, are derived in closed form in such a manner as to approximate their tabulated values given in Refs. 6 and 7. The starting point in the derivation is to develop formulas relating the thermodynamic variables p, T, ρ, Z, h, and S which will (1) approximate the tabulated values and (2) satisfy the thermodynamic relationships

$$p = RZ\rho T$$

and

$$T\,dS = dh - \frac{dp}{\rho}$$

It facilitates the development of the results to combine the previous two equations with the postulated relationships

$$\frac{h}{R} = f_1(T,Z)$$

$$p = f_2(T,Z)$$

and the identities

$$dS = \frac{\partial S}{\partial T}\,dT + \frac{\partial S}{\partial Z}\,dZ$$

and

$$\frac{\partial}{\partial Z}\left(\frac{\partial S}{\partial T}\right) = \frac{\partial}{\partial T}\left(\frac{\partial S}{\partial Z}\right) \qquad \text{(IV-1)}$$

which yields

$$\frac{\partial}{\partial T} \ln p = \frac{1}{T^2}\frac{\partial}{\partial Z}\frac{h}{R} \qquad \text{(IV-2)}$$

as a differential relationship which must be satisfied by the assumed empirical relationship. At this point the remaining details of the derivation become peculiar to the particular gas being considered.

AIR THERMODYNAMIC FUNCTIONS

Let the static enthalpy have the functional form

$$\frac{h}{R} = f(T) + (Z - 1)\,g(T)$$

When this is substituted into Eq. (IV-2) the integrated result is

$$p = F(Z)\, e^{\int \frac{g(T)}{T^2}\, dT}$$

The arbitrary functions appearing in the two previous equations are evaluated by matching the exact values in the higher range of temperatures representative of MHD operation. However, the results are insufficiently accurate at lower temperature values. In order to extend the range of validity a separate empirical fit is performed to yield comparable low temperature accuracy while at the same time rendering all the thermodynamic functions continuous (as functions of both p and T) at a matching temperature. For the sake of simplicity the low temperature formula for enthalpy (that is used when $T < T_{match}$) is not required to satisfy the entropy condition of integrability (Eq. (IV-1)). Thus, the solution of the equations of motion for an adiabatic, reversible, flow when obtained using these functions is exactly isentropic when $T > T_{match}$, but only approximately so (typically in error by 1 percent) when $T < T_{match}$. The results are:

$T \gtrless T_{match}$

$$\frac{\rho}{\rho_\infty} = 4.05 \times 10^4 \frac{(1.2 - Z)}{(Z - 1)^2} e^{-\frac{56,500}{T}}$$

$T > T_{match}$

$$\frac{h}{R} = 4.96T + (Z - 1)(56,500 + T) - 2000$$

$$\frac{S}{R} = 3.96 \ln T + (Z - 1)\left(1 + \frac{56,500}{T}\right) - \ln \rho - 0.2 \ln (1.2 - Z) - 0.919146$$

$T < T_{match}$

$$\frac{h}{R} = (a_1 + a_2 T)T + (Z - 1)(56,500 + T) + a_3$$

$$\frac{S}{R} = (a_1 - 1) \ln T + 2a_2 T + (Z - 1)\left(1 + \frac{56,500}{T}\right) - \ln \frac{\rho}{\rho_\infty} - 0.2 \ln (1.2 - Z) + a_4$$

Solve for T_{match} from

$$a_1 + 2a_2 T_{match} = 4.96$$

$$\begin{aligned} a_1 &= 3.322661 \\ a_2 &= 3.24611\text{x}10^{-4} \\ a_3 &= 64.6859 \\ a_4 &= 9.9744 \end{aligned}$$

The values of a_1 and a_2 are determined from the observation that at sufficiently low temperatures $\frac{h}{RT}$ versus T is virtually a linear function; i. e., $\frac{h}{RT} \approx a_1 + a_2 T$. The value of T_{match} is determined by requiring continuity in C_p; a_3 and a_4 are given by fulfilling continuity of h/R and S/R, respectively, at the matching temperatures.

NITROGEN THERMODYNAMIC FUNCTIONS

A single set of expressions is obtained for the entire range of interest by postulating the expressions for h/R and Z given below where the constants are evaluated by optimizing the accuracy of C_p.

$$\frac{h}{R} = \left[C_1 + \frac{\theta_v}{(e^{\theta_v/T} - 1)T} + C_2 T + Z\right] T + C_3 (Z - 1)$$

$$Z - 1 = C_5 \left[\frac{\frac{p}{p_\infty}}{C_4 T}\right]^{-C_8} e^{\left(-\frac{C_7}{T}\right)}$$

$$\frac{S}{R} = (1 + C_1) \ln T + 2C_2 T - \ln \frac{p}{p_\infty} + (Z - 1)\left(1 + \frac{C_3}{T} + \frac{1}{C_8}\right) + \frac{\theta_v}{2T} \coth \frac{\theta_v}{2T} - \ln\left(\sinh \frac{\theta_v}{2T}\right) + C_8$$

$$\begin{aligned} C_1 &= 2.5 & C_8 &= .496404 \\ C_2 &= 7.57143\text{x}10^{-6} & C_7 &= 55830.65 \\ C_3 &= C_7/C_6 & C_8 &= 2.38 \\ C_4 &= 3.66099\text{x}10^{-3} & \theta_v &= 3340 \\ C_5 &= 276.6027 \end{aligned}$$

APPENDIX V
ELECTRIC CURRENT DENSITY IN FARADAY CHANNELS

Since the boundary conditions for the electrical portion of the problem of flow through Faraday channels is posed in terms of current (on the insulator portion of the walls $j_n = 0$, along the electrode section $j_n(x)$ is specified, and at the upstream and downstream ends of the region of computation $\vec{j} = 0$), it is natural to solve a differential equation for a current stream function (rather than an electric potential) since this results in the boundary conditions being of the Dirichlet type. The derivation of this equation is performed by substituting $\vec{E}$ as a function of $\vec{j}$, from Ohm's law, into the steady-state form of Faraday's law, and then substituting a current stream function for $\vec{j}$ from conservation of current. The analytical expressions of these statements are

$$\begin{aligned} \nabla \times \vec{E} &= 0 \\ \sigma E_s &= j_s + \omega\tau\, j_n \\ \sigma(E_n - qB) &= -\omega\tau\, j_s + j_n \\ W\vec{j} &= \nabla \times [0,\ 0,\ \Psi] \end{aligned} \tag{V-1}$$

Since the curl operation is invariant under an orthonormal curvilinear coordinate transformation it follows that

$$Wj_s = \frac{\partial \Psi(s,n)}{\partial n}$$

and

$$Wj_n = -\frac{\partial \Psi(s,n)}{\partial s}$$

When a further coordinate transformation to the von Mises variables, with which the problem is solved, is introduced the result is

$$Wj_s = \left(-\frac{\partial y}{\partial s}\frac{\partial}{\partial x} + \frac{d\psi}{dn}\frac{\partial}{\partial \psi}\right) \Psi(x,\psi)$$

and

$$Wj_n = \left(-\frac{\partial x}{\partial s}\frac{\partial}{\partial x}\right) \Psi(x,\psi) \tag{V-2}$$

The combination of Eqs. (V-1) and (V-2) results in the elliptic differential equation

$$\Psi_{xx} + A_2\Psi_{\psi\psi} + A_3\Psi_x + A_4\Psi_\psi = A_5 + A_6\Psi_{x\psi}$$

where

$$A_2 = \left(\frac{d\psi}{dn}\right)^2$$

$$A_3 = -\left[\omega\tau\left(\frac{\partial x}{\partial s}\right)^2 \frac{\partial^2 y}{\partial x^2} + \frac{\frac{\partial}{\partial x} W\sigma}{W\sigma} + W\sigma \frac{d\psi}{dn}\frac{\partial}{\partial\psi}\left\{\frac{\omega\tau\frac{\partial x}{\partial s} + \frac{\partial y}{\partial s}}{W\sigma}\right\}\right]$$

$$A_4 = W\sigma\left[\left(\omega\tau\frac{\partial x}{\partial s} - \frac{\partial y}{\partial s}\right)\frac{\partial}{\partial x}\left(\frac{\frac{d\psi}{dn}}{W\sigma}\right) + \frac{d\psi}{dn}\frac{\partial}{\partial\psi}\left(\frac{\frac{d\psi}{dn}}{W\sigma}\right)\right] + \frac{\partial x}{\partial s}\frac{\partial\omega\tau}{\partial x}\frac{d\psi}{dn}$$

$$A_5 = W\sigma\frac{\partial x}{\partial s}\frac{\partial}{\partial x}qB$$

$$A_6 = 2\frac{\partial y}{\partial s}\frac{\partial\psi}{\partial n}$$

The term containing the mixed derivative is included on the right-hand side where it can be treated as a known quantity in the method of successive approximations that is used to simultaneously solve the coupled gas dynamic-electrical problem. The motivation for proceeding in this manner is that the inclusion of mixed derivative terms on the left-hand side adds complexity to the finite difference method of solution.

APPENDIX VI
ELECTRIC POTENTIAL IN HALL CHANNELS

The boundary conditions for the electrical portion of the problem of flow through the Hall channel considered in this report (two-terminal operation with equipotential surfaces on the ends:

$$V_y = 0 \text{ and } j_n(x)\Big|_{\substack{\text{upper}\\\text{wall}}} = j_n(x)\Big|_{\substack{\text{lower}\\\text{wall}}}$$

in the electrode region) are such that it is natural to solve a differential equation for an electric potential (rather than for a current stream function) since this results in the boundary conditions on the ends being of the Dirichlet type. The derivation of this equation is performed by substituting $\vec{j}$ as a function of $\vec{E}$, from Ohm's law, into the equation describing conservation of current, and then substituting an electric potential for $\vec{E}$ as a consequence of Faraday's law. The analytical expressions of these statements are

$$\begin{aligned} \nabla \cdot W\vec{j} &= 0 \\ j_s &= \frac{\sigma}{1 + (\omega\tau)^2}\left[E_s - \omega\tau(E_n - qB)\right] \\ j_n &= \frac{\sigma}{1 + (\omega\tau)^2}\left[E_n - qB + \omega\tau\, E_s\right] \\ \vec{E} &= -\nabla\varphi \end{aligned} \qquad \text{(VI-1)}$$

Since the gradient operation is invariant under an orthonormal curvilinear coordinate transformation, it follows that

$$E_s = -\frac{\partial\varphi(s,n)}{\partial s}$$

$$E_n = -\frac{\partial\varphi(s,n)}{\partial n}$$

When a further coordinate transformation to the von Mises variables is introduced, the result is

$$\begin{aligned} E_s &= \left(-\frac{\partial x}{\partial s}\frac{\partial}{\partial x}\right)\varphi(x,\psi) \\ E_n &= \left(\frac{\partial y}{\partial s}\frac{\partial}{\partial x} - \frac{d\psi}{dn}\frac{\partial}{\partial\psi}\right)\varphi(x,\psi) \end{aligned} \qquad \text{(VI-2)}$$

The combination of Eqs. (VI-1) and (VI-2) results in the elliptic differential equation

$$A_1\varphi_{xx} + A_2\varphi_{\psi\psi} + A_3\varphi_x + A_4\varphi_\psi = A_5 + A_6\varphi_{x\psi}$$

where

$$A_1 = \frac{W\sigma}{1 + (\omega\tau)^2}$$

$$A_2 = \frac{W\sigma}{1 + (\omega\tau)^2} \left(\frac{d\psi}{dn}\right)^2$$

$$A_3 = -\frac{W\sigma}{1 + (\omega\tau)^2} \frac{d\psi}{dn} \frac{\partial}{\partial\psi}\left(\frac{\partial y}{\partial s}\right) + \frac{\partial}{\partial x}\left(\frac{W\sigma}{1 + (\omega\tau)^2}\right)$$

$$+ \frac{d\psi}{dn}\left[\frac{\partial x}{\partial s} \frac{\partial}{\partial\psi}\left(\frac{W\sigma\ \omega\tau}{1 + (\omega\tau)^2}\right) - \frac{\partial y}{\partial s} \frac{\partial}{\partial\psi}\left(\frac{W\sigma}{1 + (\omega\tau)^2}\right)\right]$$

$$A_4 = \frac{W\sigma}{1 + (\omega\tau)^2}\left[-\frac{\partial y}{\partial s} \frac{\partial}{\partial x}\left(\frac{d\psi}{dn}\right) + \frac{d\psi}{dn} \frac{\partial}{\partial\psi}\left(\frac{d\psi}{dn}\right)\right.$$

$$+ \frac{d\psi}{dn}\left[-\frac{\partial x}{\partial s} \frac{\partial}{\partial x}\left(\frac{W\sigma\ \omega\tau}{1 + (\omega\tau)^2}\right) - \frac{\partial y}{\partial s} \frac{\partial}{\partial x}\left(\frac{W\sigma}{1 + (\omega\tau)^2}\right)\right.$$

$$\left.\left. + \frac{d\psi}{dn} \frac{\partial}{\partial\psi}\left(\frac{W\sigma}{1 + (\omega\tau)^2}\right)\right]\right]$$

$$A_5 = \frac{\partial x}{\partial s} \frac{\partial}{\partial x}\left[\frac{W\sigma\ \omega\tau}{1 + (\omega\tau)^2}\ qB\right] + \frac{\partial y}{\partial s} \frac{\partial}{\partial x}\left[\frac{W\sigma}{1 + (\omega\tau)^2}\ qB\right]$$

$$- B \frac{d\psi}{dn} \frac{\partial}{\partial\psi}\left[\frac{W\sigma}{1 + (\omega\tau)^2}\ q\right]$$

$$A_6 = 2 \frac{\partial y}{\partial s} \frac{W\sigma}{1 + (\omega\tau)^2} \frac{d\psi}{dn}$$

APPENDIX VII
DIRECT METHOD OF SOLUTION OF FINITE DIFFERENCE EQUATIONS

The partial differential equations for electric current stream function and potential that are derived in Appendixes V and VI are written in implicit finite difference forms using central differences as approximations to the derivatives. The resulting matrix equation is block tridiagonal; i. e., the partitioned form of the coefficient matrix is tridiagonal. The methods that have been proposed in the literature for solving such an equation (i. e., a system of linear algebraic relationships) fall into the general categories of iterative, direct, and block iterative which is a hybrid of the first two methods. Several iterative schemes have been applied by various authors to the solution of implicit finite difference equations when their numerical properties were sufficiently simple. An extensive test of block iterative techniques in the course of the analysis that forms the subject of this report was made and it was found that iterative methods are incapable of solving the electrical boundary value problems that are described herein. The problems were ultimately solved by the use of a direct method on a numerical gridwork whose size is limited only by the available memory of the digital computer being used. It has been shown by substitution that the values computed for the unknown variable invariably satisfy the given matrix equation. That the success of such an approach was not a priori obvious is explained by the well-known fact that the finite word length of a computer results in an accumulation of truncation error that, in general, precludes the successful employment of a direct method. However, it was found that one particular variant of the direct algorithm proposed by Schechter in Ref. 4 has the capability of negating truncation error accumulation. The method proceeds by accomplishing a forward elimination with a conventional factorization of the coefficient matrix into a product of lower and upper diagonal matrices. The distinguishing characteristic of the Schechter method is that instead of performing the entire backsweep by obvious recurrence relations (which would invariably lead to numerical instabilities), the backsweep operation is periodically interspersed with formulas for the unknowns that involve the use of intermediate calculations performed and stored in the computer memory during the forward elimination process. Thus by limiting the number of consecutive applications of straightforward recurrence relationships, it has been found possible in all cases to perform the calculations within numerical stability boundaries. The efficacy of the method is attributable to this property and also to the simplicity of the algorithm, which is presented below in the notation of Ref. 4. In order to display this simplicity the entire matrix algebra necessary to effect the solution (given by Eqs. (VII-1) through (VII-5)) is presented first, then a definition of terms is given.

FORWARD ELIMINATION

$$A_1 \equiv M_1$$

$$A_n \equiv M_n - D_n A_{n-1}^{-1} E_{n-1}, \quad 1 < n \leq q_k \qquad \text{(VII-1)}$$

$$\{y_1\} \equiv \{g_1\}$$

$$\{y_n\} \equiv \{g_n\} - D_n A_{n-1}^{-1} \{y_{n-1}\}, \quad 1 < n \leq q_k \qquad \text{(VII-2)}$$

BACKSWEEP

$$\{v_{q_k}\} \equiv A_q^{-1} \{y_{q_k}\} \qquad \text{(VII-3)}$$

$$\{v_{n-1}\} \equiv D_n^{-1} \left\{ \{g_n\} - M_n \{v_n\} - E_n \{v_{n+1}\} \right\} \qquad \text{(VII-4)}$$

$$\{v_n\} \equiv A_n^{-1} \{y_n\} - A_n^{-1} E_n \{v_{n+1}\} \qquad \text{(VII-5)}$$

The braces around the terms indicate vector matrices of length p, and the other matrices are rectangular.

The symbolism used in Eqs. (VII-1) through (VII-5) (which is the same as that used in Ref. 4) is related to the physical problem as follows. Denote the first upstream column of gridpoints by n = 1 and the last downstream column by n = q_k where k denotes the number of changes in the number of unknowns to be solved for on the individual columns. Let p_r denote the number of rows on column q_r.

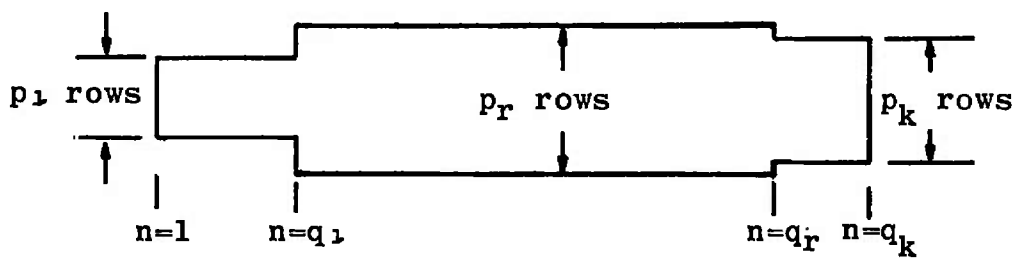

Physical Array

As is well known the finite difference relations for a linear second-order partial differential equation without mixed derivatives can be written in partitioned matrix form as

$$\begin{bmatrix} M_1 & E_1 & & & \\ D_2 & M_2 & E_2 & & \\ & \ddots & \ddots & \ddots & \\ & & D_n & M_n & E_n \\ & & & \ddots & \ddots \\ & & & & D_{q_k} \quad M_{q_k} \end{bmatrix} \begin{Bmatrix} v_1 \\ v_2 \\ \vdots \\ v_n \\ \vdots \\ v_{q_k} \end{Bmatrix} = \begin{Bmatrix} g_1 \\ g_2 \\ \vdots \\ g_n \\ \vdots \\ g_{q_k} \end{Bmatrix} \qquad \text{(VII-6)}$$

where D_n, M_n, E_n are matrices with the same number of rows, E_n, M_{n+1}, D_{n+2} have the same number of columns, and the M_n are square (p_r x p_r). The vectors $\{v_n\}$ are the unknowns; in the context of this report these are successive approximations to the current stream function (Faraday channels) or electrical potential (Hall channels).

The derivation of the solution algorithm is performed as follows. Denote the coefficient matrix by Q; Eq. (VII-6) can then be written as $Q\{v\} = \{g\}$. Equation (VII-7) results from the factorization of the coefficient matrix Q into a product of lower and upper diagonal matrices $Q = LU$.

$$[L] \qquad\qquad [U] \qquad\qquad \{v\} = \{g\}$$

$$Q\{v\} = \begin{bmatrix} I & & & \\ [D_2 A_1^{-1}] & I & & \\ & \ddots & \ddots & \\ & & [D_{q_k} A_{q_k-1}^{-1}] & I \end{bmatrix} \begin{bmatrix} A_1 & E_1 & & \\ & A_2 & E_2 & \\ & & \ddots & \ddots \\ & & & A_{q_k} \end{bmatrix} \begin{Bmatrix} v_1 \\ v_2 \\ \vdots \\ v_{q_k} \end{Bmatrix} = \begin{Bmatrix} g_1 \\ g_2 \\ \vdots \\ g_{q_k} \end{Bmatrix}$$

(VII-7)

Equation (VII-2) is obtained by solving for $\{y\}$ from $\{y\} = U\{v\}$ and $L\{y\} = \{g\}$. Equation (VII-3) is obtained from the last row of $U\{v\} = \{y\}$. Equation (VII-4) is obtained by rewriting the nth row of $Q\{v\} = \{g\}$

$$D_n \left\{v_{n-1}\right\} + M_n \left\{v_n\right\} + E_n \left\{v_{n+1}\right\} = \left\{g_n\right\}$$

Equation (VII-5) is obtained by solving for $\left\{v_n\right\}$ from the nth row of $U\left\{v\right\} = \left\{y\right\}$, which is $A_n \left\{v_n\right\} + E_n \left\{v_{n+1}\right\} = \left\{y_n\right\}$. The reader is referred to Ref. 4 for additional details of the matrix algebra that are required.

APPENDIX VIII

TABLE I
INITIAL CONDITIONS—UNIFORM AND NONUNIFORM INLET PROFILES, ACCELERATOR A

The initial conditions listed below are values at the entrance to the electrode section that would result from an isentropic expansion through the channel.

UNIFORM INITIAL PROFILES	NONUNIFORM INITIAL PROFILES
Assumptions: $p/p_\infty = 0.5$	Assumptions: $p/p_\infty = 0.5$
$M = 1.6$	$M = 1.6$
	M is uniform in transverse direction
	T is a quadratic function of the transverse coordinate
	$T_{\text{¢}} = 1.5 \times T_{wall}$
$H = 5.4168\ (10^6)$ m^2/sec^2	$T_{\text{¢}} = 3600°K$
The assumptions imply values of velocity and temperature.	The assumptions imply $H_{avg} = 5.4168\ (10^6)$ m^2/sec^2, and a velocity profile.

TABLE II
INITIAL CONDITIONS—UNIFORM AND NONUNIFORM INLET PROFILES, ACCELERATOR B

The initial conditions listed below are values at the entrance to the electrode section that would result from an isentropic expansion through the channel.

UNIFORM INITIAL PROFILES

Assumptions:

- $p/p_\infty = 0.5$
- $u = 3000$ m/sec
- $T = 3400°K$

The assumptions imply

$$\dot{m} = 0.7158 \text{ kg/sec}$$

$$H = 10.262\ (10^6)\ m^2/sec^2$$

NONUNIFORM INITIAL PROFILES

Assumptions:

- $p/p_\infty = 0.5$
- p_o is uniform in transverse direction
- H is a quadratic function of the transverse coordinate
- $H_{\text{℄}} = 1.5 \times H_{wall}$
- $\dot{m} = 0.7158$ kg/sec
- $H_{avg} = 10.262\ (10^6)\ m^2/sec^2$

The assumptions imply profiles of velocity and temperature.

TABLE III
INITIAL CONDITIONS—NONUNIFORM INLET PROFILES, ACCELERATOR C

The initial conditions listed below are values at the entrance to the electrode section that would result from an isentropic expansion through the channel.

The following one-dimensional values are from Ref. 11, Run 1323:

$$p/p_\infty = 4.7$$

$$T_{1\text{-dim}} = 3100°K$$

$$u_{1\text{-dim}} = 2960 \text{ m/sec}$$

The criterion for choosing the following relationships is explained in Ref. 5.

$$\frac{T - T_{wall}}{T_{\text{¢}} - T_{wall}} = 1 - \left(\frac{y}{\frac{d}{2}}\right)^2$$

$$\frac{u - u_{wall}}{u_{\text{¢}} - u_{wall}} = \left[1 - \left(\frac{y}{\frac{d}{2}}\right)^2\right]^{1/2}$$

$$\frac{T_{1\text{-dim}} - T_{wall}}{T_{\text{¢}} - T_{wall}} = \frac{2}{3}$$

$$\frac{u_{1\text{-dim}} - u_{wall}}{u_{\text{¢}} - u_{wall}} = \frac{2}{3}$$

$$\frac{T_{\text{¢}}}{T_{wall}} = 1.22$$

$$\frac{u_{\text{¢}}}{u_{wall}} = 1.5$$

UNCLASSIFIED

Security Classification

DOCUMENT CONTROL DATA - R & D

(Security classification of title, body of abstract and indexing annotation must be entered when the overall report is classified)

1 ORIGINATING ACTIVITY (Corporate author) Arnold Engineering Development Center ARO, Inc., Operating Contractor Arnold Air Force Station, Tennessee 37389	2a. REPORT SECURITY CLASSIFICATION UNCLASSIFIED 2b. GROUP N/A

3 REPORT TITLE

TWO-DIMENSIONAL FLOW CALCULATIONS IN THE ELECTRIC FIELD PLANE FOR LINEAR MHD CHANNELS

4. DESCRIPTIVE NOTES (Type of report and inclusive dates)

Final Report, July 5, 1966 to June 30, 1970

5. AUTHOR(S) (First name, middle initial, last name)

Paul W. Johnson, ARO, Inc.

6. REPORT DATE September 1971	7a. TOTAL NO. OF PAGES 61	7b. NO OF REFS 12
8a. CONTRACT OR GRANT NO. F40600-72-C-0003 b. PROJECT NO. 8950 c. Program Element 62405334 d.	9a. ORIGINATOR'S REPORT NUMBER(S) AEDC-TR-71-181 9b. OTHER REPORT NO(S) (Any other numbers that may be assigned this report) ARO-PWT-TR-71-118	

10 DISTRIBUTION STATEMENT

Approved for public release; distribution unlimited.

11. SUPPLEMENTARY NOTES Available in DDC.	12. SPONSORING MILITARY ACTIVITY Arnold Engineering Development Center, AFSC, Arnold Air Force Station, Tennessee 37389

13. ABSTRACT

The two-dimensional, steady, compressible, inviscid flow of ionized gas through linear, segmented electrode, magnetohydrodynamic (MHD) channels is computed in the plane of the applied electric field. The solutions obtained for the gas dynamic and electrical quantities satisfy the coupled fluid mechanical conservation laws and Maxwell's equations at all points of the flow field simultaneously. The nonuniform profiles which are obtained include the effects of transverse variations in incoming gas dynamic profiles, local Hall currents in Faraday channels, transverse currents in Hall devices, and axial magnetic field gradients.

DD FORM 1 NOV 65 1473

UNCLASSIFIED

Security Classification

14. KEY WORDS	LINK A		LINK B		LINK C	
	ROLE	WT	ROLE	WT	ROLE	WT
magnetohydrodynamics						
mathematical models						
supersonic flow						

AFSC
Arnold AFS Tenn